STRUCTURED STYRENIC POLYMER MICROSPHERES BY PRECIPITATION POLYMERIZATION

By YUQING ZHAO, B.Sc.

A Thesis Submitted to the School of Graduate Studies

In Partial Fulfillment of the Requirements

For the Degree Master of Science

McMaster University

MASTER OF SCIENCE (2015) McMaster University

(Chemistry and Chemical Biology) Hamilton, Ontario

TITLE: Structured Styrenic Polymer Microspheres by Precipitation Polymerization

AUTHOR: Yuqing Zhao, B.Sc. (Hong Kong Baptist University, HK)

SUPERVISOR: Dr. Harald Stöver

NUMBER OF PAGES: VIII, 79, VII

ACKNOWLEDGEMENT

I hereby express my deepest gratitude and respect to my supervisor, Dr. Harald Stöver, for his knowledgeable insights and continuous encouragement. I have most appreciated the considerate mentorship and enthusiastic environment Dr. Stöver provides in my way towards the nature of science.

I would like to show sincere thanks to my group members for all their help and support in academic and life. With all my colleagues accompanying me, I could have completed my Master's research with memorable experience. Many thanks to: Rachelle, Alison, Samantha, Jing, Jingwen (visiting student) and Nick. I am grateful to Dr. Nick Burke, for his continuously offering great help and guidance, with which I have extended my horizon and gained in-depth understanding in polymer science.

I am grateful for all the help received from Marcia Reid and McMaster University Electron Microscopy facility, whose expertise supports the TEM part in my research.

I would also like to acknowledge Natural Sciences and Engineering Research Council of Canada (NSERC) CREATE Program for financial support.

Finally, I would like to thank my friends and my family. Without your friendship, love, and encouragement, I wouldn't have a lively life.

TABLE OF CONTENTS

LIST OF FIGURES & TABLES

Chapter One

Chapter Two

Chapter Threee

Chapter Four

Chapter Five

ABSTRACT

Precipitation polymerization is a unique method that produces narrow-disperse, uniform polymer particles with clean surfaces. In this research, internally structured poly(divinylbenzene-*co*-chloromethylstyrene) polymer microspheres were prepared by thermal imprinting precipitation polymerization. The influence of thermal profiles and the monomer/crosslinker feed ratio on the resulting core-shell microspheres were explored by optical and transmission electron microscopy, and potential route to extend this technique to other polymer system was discussed. Further surface functionalization of this type of particles was demonstrated by substitution of chlorine with cysteine, a good and hydrophilic nucleophile. Narrow-disperse, hydrophilic particles may in future serve as components of synthetic extracellular matrices used in exploring cell-matrix interactions in a 3D context.

CHAPTER ONE

1 Introduction of Polymer Microspheres

1.1 Introduction

The 3D structure of small dispersed systems in nature is often governed by the desire to minimize interfacial tension. Examples of dispersed systems include water droplets in air, oil droplets in water, and even some living cells and their internal compartments. Colloid science deals with the formation and properties of many types of small particles, including spherical polymer particles. Polymer micro- and nanoparticles can be formed by a range of heterogeneous polymerizations including suspension, emulsion, dispersion and precipitation polymerization. These particles may be colloidally stabilized by electrostatic, steric, and electrosteric forces. In precipitation polymerization, steric stabilization through a self-renewing surface gel layer can prevent coagulation of particles, and can lead to stabilizer-free, narrow-disperse spherical particles with controllable surface chemistry.

1.2 Traditional Heterogeneous Polymerizations

Traditionally, there are four polymer production methods: bulk polymerization, solution polymerization, suspension polymerization and emulsion polymerization.

Bulk polymerization requires only monomer and initiator, and can hence lead

to very pure products. However, process control, thermal management and product work-up are challenging on large scales, so that bulk polymerization is usually restricted to low viscosity polymers, such as lubricants, plasticizers and adhesives.

In solution polymerization, monomer and initiator dissolve and react in a solvent, with the product polymer remaining in solution. Isolation of the product, as well as recovery of the solvent, can become prohibitively expensive on large scales.

Heterogeneous polymerizations including suspension, emulsion, dispersion and precipitation polymerizations were developed in part to overcome such issues. They may start as two-phase or homogeneous mixtures, and the polymers are obtained in form of dispersed particles at the end of polymerization. These particles have different sizes, size distributions, and sometimes shapes. Generally, suspension polymerization produces polydisperse particles with diameters in the range from 5 to 1000 μm,[2] while emulsion polymerization produces monodisperse particles with diameters of about 100 to 1000 nm.[2] The particles diameters produced by dispersion and precipitation polymerizations lie between these above two methods.[2] Classical precipitation polymerization leads to irregular particle shapes, though recent developments led to formation of narrow disperse spherical particles in presence of crosslinking under marginal solvent conditions. These four main methods are discussed in more detail below.

1.2.1 Suspension Polymerization

Suspension polymerization involves monomer droplets suspended in an immiscible liquid, usually water. The initiator is soluble in the monomer, and polymerization occurs in each monomer droplet which acts as a “microbulk” polymerization reactor, with efficient heat transfer into the continuous phase. Hydrophobic monomer-initiator droplets are kept in suspension by continuous mechanical stirring and use of stabilizers like poly(vinyl alcohol), and are converted into polymer beads. The overall cycle of particle shearing and aggregation during polymerization is shown in Scheme 1.2.1[1]. It is useful for production of particles with broad size distribution from about 5 to 1000 microns, which can be used as e.g. ion exchange resins and chromatographic separation media. If narrow disperse particles are required, sieves are needed to classify the particles.

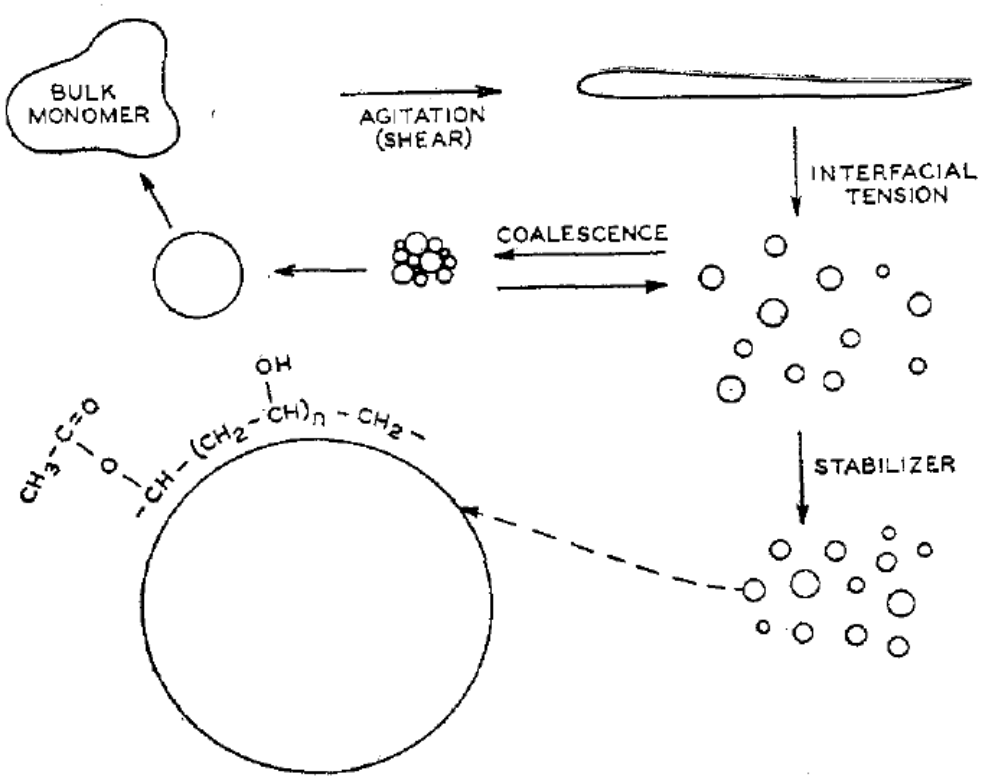

Scheme 1.2.1 Schematic diagram of states of dispersion in suspension polymerization of technical divinylbenzene[1] (Reprinted with permission from Ref.1, Copyright © 1951, American Chemical Society)

The average size of monomer droplets and the size distribution can be affected by the ratio of monomer volume to medium, stabilizer concentration, stirring speed and viscosities of both phases. Quantitative expressions for these relationships have been reported.[2] Generally, the particle size is proportional to monomer loading[3] and inversely proportional to stirring speed[4] and stabilizer concentration[1]. Another variable is the particle morphology which is of particular interest in applications as ion exchange resin and polymeric supports.[3, 5, 6] Whether the surface is smooth or porous depends on the solubility of the formed polymers in the monomer phase. If the polymer is soluble in its monomer mixture, smooth surface

particles will be produced, and vice versa. Diluents called porogens may be added to the dispersed phase to generate a wide range of porosities.[5, 7] Suspension polymerization is a mature technology, with renewed interest on large scale production of polymer beads with narrow size distribution, as well as in forming core-shell[8] and hollow particles.[9].

1.2.2 Emulsion Polymerization

Emulsion polymerization is similar to suspension polymerization, as shown in Scheme 1.2.2[10]. The process is typically based on organic monomer droplets, stabilized by emulsifier or surfactant and dispersed in a continuous water phase, with the radical initiator dissolved in the aqueous continuous phase. The polymerization starts when partially water-soluble monomer diffuses into the aqueous media and reacts with the initiator radicals. The resulting oligomers, together with some of the monomer, partition into surfactant micelles where most of the polymerization takes places. Polymerization continues and consumes monomers inside micelles, resulting in further monomer migration from monomer droplets and aqueous phase to micelles with active polymer chains. Termination occurs when a second radical enters the micelle with propagating polymer chain. At the end of the polymerization, most monomer droplets are consumed, while the micelles have turned into polymer particles. Both molecular weight and polymerization rate can be

controlled through surfactant concentration.

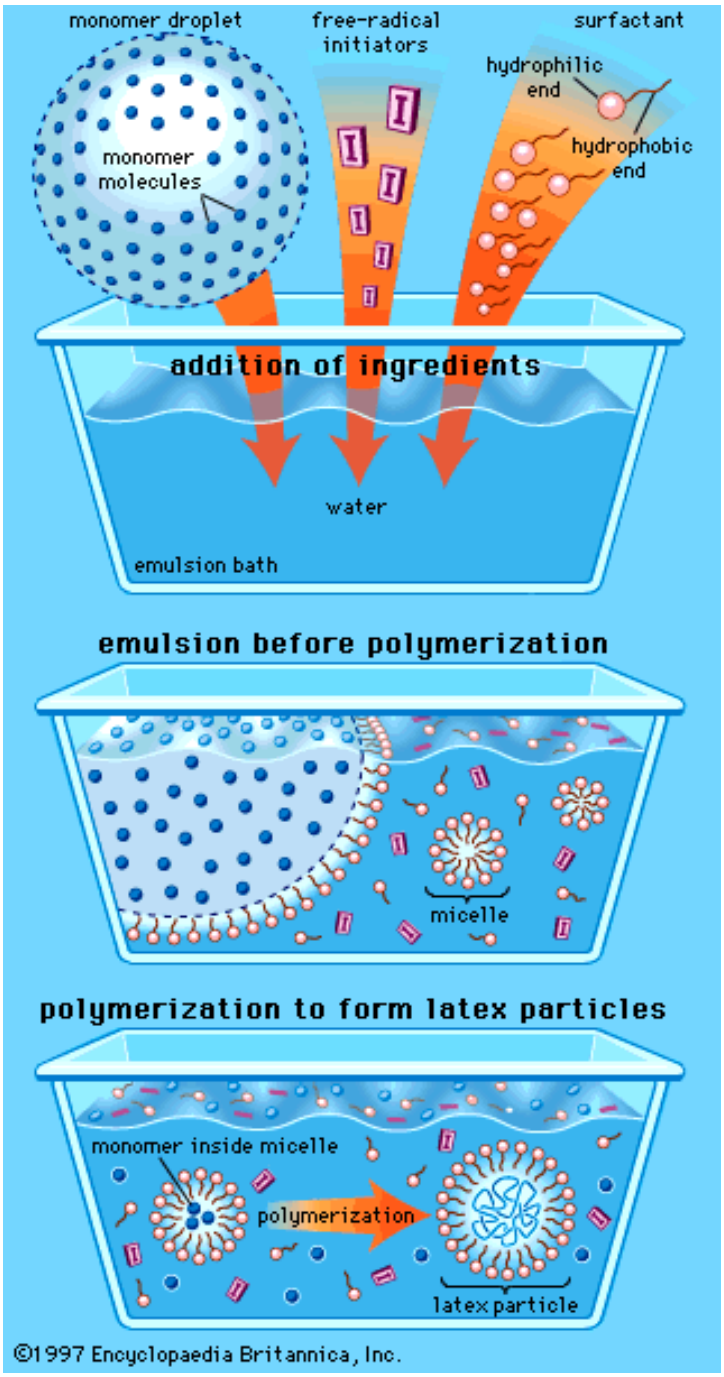

Scheme 1.2.2 Schematic diagram of emulsion polymerization method[10]

The diameter of the final emulsion polymer particles is usually in the range of 100-1000 nm. As the polymerization occurs in micelles, final particle size does not

depend on the size of the initial monomer droplets[2], but on the solubility of monomer(s) in the continuous phase, emulsifier concentration and polymerization temperature. A great deal of work focusing on mechanism and kinetics, has been reviewed.[11] In Gardon's study, the particle size was controlled by varying the nucleation rate (polymerization rate), and the results showed that particle size is inversely proportional to the polymerization temperature.[12] Detailed experiments revealed that an increasing rate of formation of radicals in the aqueous phase, leads to a larger number of nuclei, and a smaller final particle size. As predicted by Smith-Ewart's theory[11], high emulsifier concentration allows formation of more micelles and hence, contributing to smaller particle size in the aqueous phase.

In emulsion polymerization, surfactant plays an important role and the corresponding critical micelle concentration (CMC) is essential for micelle formation in solution. CMC is varied among polymers and micelles are formed when surfactant concentration increases to CMC point or exceeds it. Other morphologies like bilayer, cylindrical or liposome are also possible formations and details are study by Israelachvili.[13] For polymerization, surfactant concentration usually are at least one order above CMC and micelles are formed with diameter about 2 -10 nm

Emulsifier-free emulsion polymerizations[14, 15] are carried out in the same way as classical emulsion polymerization, but without surfactants and micelles

formed during the polymerization from ionic initiators. The colloid is stabilized by the ionic groups of the initiator residues on their surface.[14]

1.2.3 Dispersion Polymerization

Unlike emulsion and suspension polymerization, dispersion polymerization starts with homogeneous conditions with monomer, initiator and colloidal stabilizer such as poly(vinylpyrrolidone), PVP, all dissolved in the medium, which is usually an organic solvent, such as ethanol. The initially formed polymer chains separate from the homogenous phase and aggregate until the formed nuclei become colloidally stabilized by adsorption of polymer chains grafted with PVP. Scheme 1.2.3[16] shows the nucleation and growth of particles in dispersion polymerization, leading to formation of particles with diameters of about 0.1 - 10 μm. The need to allow the stabilizing graft copolymers to remain at the surface of the growing particles prevents the use of crosslinkers in dispersion polymerization.

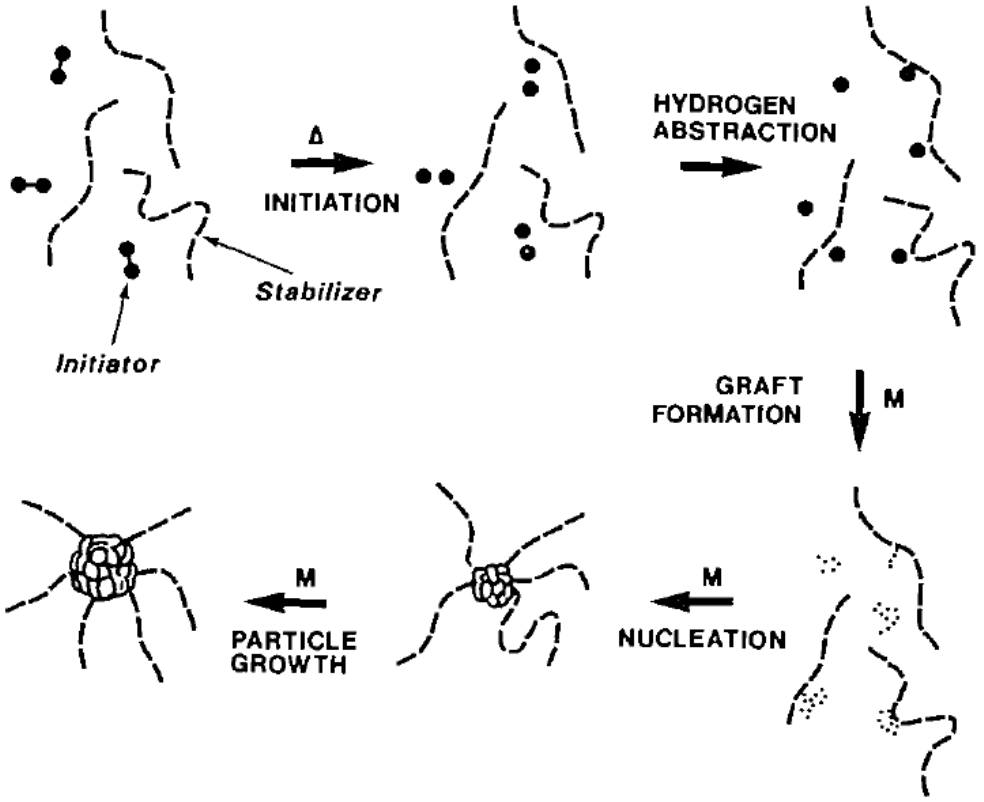

Scheme 1.2.3 Schematic presentation of nucleation and particle growth in dispersion polymerization[16] (Reprinted with permission from Ref.15, Copyright © 1985, NRC Research Press or its licensors)

The factors controlling particle size include polymer solubility; stabilizer type, molecular weight and concentration; temperature, and solvent properties.[16] A study by Lok and Ober[16] was focused on polystyrene particles formed using cellulosic stabilizers in different solvent combinations. Adding poorer (e.g., more polar) solvents, led to smaller particles. Hansen solubility parameters offer insights into the fundamentals of polymer-solvent interactions and their effects on particle colloidal stability and size. Paine described how Hansen's approach considers three components: the dispersion term (δ_d), hydrogen bonding term (δ_h) and polarity term (δ_p), instead of the single Hildebrand solubility parameter.[17] In addition,

temperature can affect particle size and size distribution[18] by influencing both thermodynamic factors like solubility, and kinetic factors such as rate of initiator decomposition[16].

Monomer and stabilizer concentration also directly affect the particle size. Polymerization of styrene with PVP stabilizer in alcoholic solvents shows that increasing initial monomer concentration results in larger particles.[19]

1.3 Precipitation Polymerization

1.3.1 Development of precipitation polymerization

Modern precipitation polymerization can produce monodisperse, crosslinked polymer microspheres, and has thus attracted increasing interest in academia, and in specialty industries. A key feature of this technique is the absence of any added stabilizer, leading to very clean particles. A systematic review of modern precipitation polymerization has been given by Möhwald et al.[20]. For a typical precipitation polymerization system, monomer and/or cross-linker and radical initiator are dissolved in solvent and polymerized as in classic solution polymerization. The growing oligomers precipitate out of the solvent when they reach their solubility limit, and crosslink to form colloidally stable nuclei that continue to grow into the final particles.[21] Colloidal stability is provided by the transient surface gel layer.

This process evolved of classical precipitation polymerizations where the monomer is soluble in the polymerization solvent, while the forming polymer precipitates out during polymerization. This method has been practiced for a long time period, and typically results in non-uniform particles[22-24]. In 1993, the preparation of monodisperse poly(divinylbenzene-55) particles (PDVB-55) by precipitation polymerization was reported.[21] In that process, DVB-55, a mixture of divinylbenzene and vinylethylbenzene isomers is polymerized with AIBN as initiator in acetonitrile to yield highly crosslinked particles with diameter ranging from 2 to 5 μm depending on reaction conditions. Subsequent papers described copolymer microspheres such as poly(divinylbenzene-*co*-maleic anhydride) (Poly(DVB-*alt*-MAn))[25, 26] in methyl ethyl ketone (MEK)/heptane mixtures and poly(chloromethlstyrene-*co*-divinylbenzene) (Poly(CMS-*co*-DVB))[27] in acetonitrile. Porous microspheres were formed by adding good cosolvents such as toluene to the reaction solvent (i.e. acetonitrile).[28]

Distillation-precipitation polymerization was reported in 2004 as an updated technique by Yang's group to produce monodisperse PDVB microspheres.[29] The distillation concentrates the reaction solution; as a result, particle formation is accelerated, reducing the reaction time to 2 hours and increasing the monomer conversion. Hydrophilic polymer microspheres like poly(ethyleneglycol dimethacrylate) (PEGMA)[30] and non-crosslinked poly(methacrylic acid)

(PMAA)[31-33] were also reported by distillation-precipitation polymerization. The formation of the PMAA particles involves hydrogen-bonding as a non-covalent linkage in the nucleation and growth process.[33]

Photoinitiated precipitation polymerization was reported by Irgum's group in 2007 [34] for DVB system with AIBN as UV-initiator in acetonitrile. UV initiation allowed the polymerization to proceed at or below room temperature in order to minimize temperature dependent side reactions, such as chain transfer.[35] Copolymerization of DVB-55 and glycidyl methacrylate can produce uniform porous microspheres.[36] In addition, monomer loading as high as 5 vol% can be used successfully.[34, 36]

'Living' radical polymerizations have been used to modify the surface chemistry of microspheres. For example, our group reported grafting of polystyrene[37] and poly(alkyl(meth)acrylates)[38] from polymer microspheres by atom transfer radical polymerization (ATRP). The 'grafting from' technique allows precise control of particle growth and surface modification.

1.3.2 Mechanism of precipitation polymerization

The mechanism of precipitation polymerization has been described by our group for poly(DVB55)[39, 40] and poly(DVB-*alt*-MAn)[26] systems. The proposed mechanism is shown in Scheme 1.3.2 for poly(DVB-*alt*-MAn)

microspheres formed in mixed solvents containing 40 % MEK and 60 % heptane. Basically, three stages are involved in the reaction process: oligomer formation, particle nucleation and particle growth.[26]

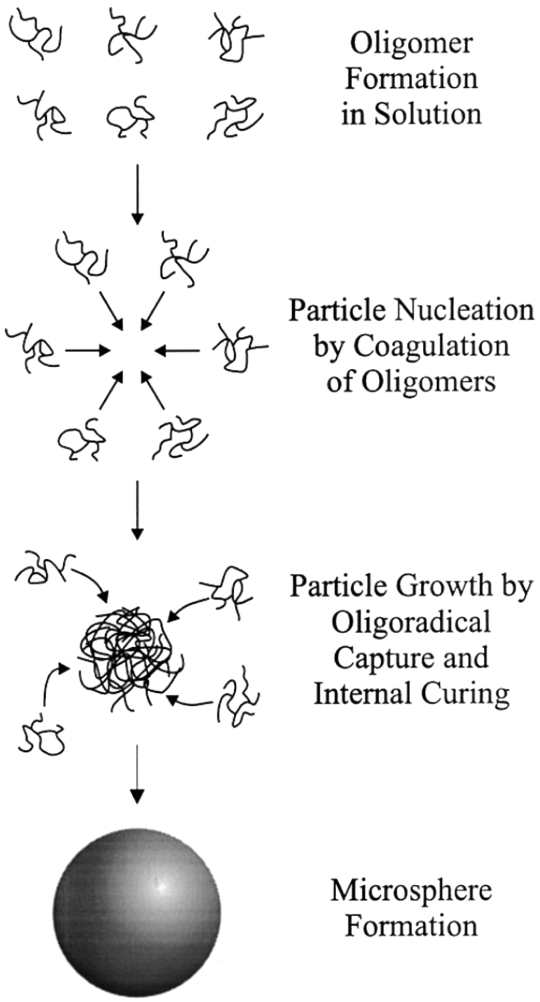

Scheme 1.3.2 Proposed mechanism for Poly(DVB-*alt*-MAn) microspheres formation in 40 % MEK and 60 % heptane[26] (Reprinted with permission from Ref.25, Copyright © 2002, American Chemical Society)

Firstly, oligomers form from monomers via classic radical polymerization in solution. These oligomers then may undergo three reactions: intermolecular aggregation, continued growth by addition of monomer, and intramolecular reaction

such as cross-linking and cyclization. All of these reactions cause a decrease of entropy of mixing with solvent and thus promote further intermolecular interactions, forming nanogels in systems with limited enthalpic polymer-solvent interactions, e.g. marginal solvents. These nanogels homocoagulate into colloidally stable microparticles that grow by further deposition of oligomers and nanogels. The interior of such polymer-based gel network continues to desolvate and collapse, driven by solvency of the continuous phase and further cross-linking.[39]

Particle nuclei are formed via homocoagulation of insoluble oligomers. Homocoagulation is supported by the fact that final particle volume for poly(DVB-*alt*-MAn) microspheres did not increase linearly with monomer concentration,[26] indicating particle nucleation is concentration dependent. Nucleation stops when all newly formed oligomers are captured by existing nuclei. The number of particles is set at this stage and particles only grow in size but not in number.

Particles grow at least in part by capturing newly-formed oligomers from solution by reaction with pendent vinyl groups or radicals on particle surfaces.[39] These captured oligomers provide steric stabilization,[26] by forming a solvated gel layer on the particle surface. Such transient gel layer prevents inter-particle coagulation and at the same time continues to crosslink, and desolvate until it becomes a part of the particles.

In heterogeneous polymerization process, there are two possible mechanisms

for particle growth: enthalpic and entropic precipitation.[40] In enthalpic precipitation, oligomers keep growing until they reach the solubility limit, phase-separate from solution and deposit on nuclei or existing particle surfaces. These nuclei and particles keep growing by capturing other nuclei and oligomers, and by incorporation of monomers. An alternative approach is entropic precipitation, which applies in precipitation polymerization. Particles grow by capturing soluble oligomers from solution through reaction with vinyl groups and radicals on the surface.[40] By continuous capturing of oligomers on the surface and further crosslinking and desolvation of the resulting gel layer, particles grow in size and transform into microspheres. The oligomers on the surface swell in the reaction medium and provide colloidal stability, suppressing inter-particle coagulation by steric stabilization.

1.3.3 Marginal solvent

Solvent selection is important for successful precipitation polymerizations. The solvent needs to be miscible with monomer and initiator, but be a poor solvent for the polymer. The selection of solvent typically depends on the monomer and polymer polarity and hydrogen-bonding ability. Flory-Huggins model and Hansen's solubility parameter have been utilized to model the relationship between Flory's parameter and particle size.[41] In our previous work, acetonitrile works for PDVB

and poly(CMS-*co*-DVB) systems[21, 27, 28, 40, 42, 43] and appropriate methyl ethyl ketone (MEK)/heptane mixtures work for PDVB and poly(DVB-*co*-MAn)[25, 26, 39]. In particular, the MEK/heptane ratio can be adjusted to match the polarity of the monomer/crosslinker mixture. Generally, near *theta* (Θ) condition solvent is required to form colloidally stable particles that grow by continuous desolvation and renewal of the transient gel layer on the particle surface.[40] The Θ condition indicates that polymer coils act as ideal chains whereby the repulsive force from excluded volume is balanced by the compressive force from surface tension of solvent. When the Θ condition is satisfied for a given polymer-solvent pair at a given temperature, the temperature is called Θ temperature, and the solvent is called Θ solvent.

The concept of marginal solvent have been discussed in detail in our previous work on DVB/MAn microspheres.[25] In that work, solvents like acetonitrile and ethanol (i.e. poor solvents for this monomer pair) lead to irregular aggregation as reaction proceeds, which was believed to result from the insufficient steric stabilization. The use of good solvents such as *n*-butanol or MEK resulted in formation of microgel rather than microspheres, indicating high affinity between polymer and solvent and swollen polymer networks that do not collapse and aggregate into particle nuclei. When MEK/heptane mixtures with 20 – 50 vol.% MEK were used, colloidally stable particles formed with low inter-particle

interaction are formed.

1.3.4 Particle size control and size distribution

Irregular shape and non-uniform size of particles may limit their application. The key to forming spherical particles is to match the three components in the system: monomer, polymer and solvent to avoid extended or secondary nucleation which can cause large size dispersities.

Increasing monomer concentration to 10 vol.% and beyond leads to higher yield of microspheres but also increases inter-particle coagulation and secondary nucleation. Particle size increases non-linearly with increasing monomer loading,[26] as increased monomer loading affects particle nucleation as well as growth.

The effect of cross-linker concentration was discussed in our previous work for PDVB and Poly(DVB-*alt*-MAn) system. At a constant MEK fraction of 25 vol.%[39], PDVB microspheres only form between 40 and 55 % actual crosslinker in the total monomer. Microspheres yields increase with increasing crosslinking level, while sizes decrease, for both DVB/MAn and the DVB/CMS systems[27].

Both overall conversion and particle size are influenced by the amount of initiator present.[21] Increased initiator concentration can lead to faster reaction, which in turn accelerates the particle growth. Also, monomer conversion grows with

initiator concentration.

1.3.5 Particle Morphology

Porous polymer particles have attracted much interest. By introducing toluene as porogenic cosolvent in the precipitation polymerization process, poly(CMS-*co*-DVB) particles can be obtained with different porosity.[26] Particles prepared with 0.1 and 0.2 mole fraction of CMS show continuous increase in porosity by elevating toluene fraction from 20 to 30 vol.%. The formation mechanism of micropores has been investigated for PDVB system[28] and can be extended to other polymer systems.

1.3.5.1 Core-shell polymeric particles

Recently, efforts have been made to form core/shell and hollow particles by various methods, as shown in Scheme 1.3.5.1[42]. Two-stage precipitation polymerization can be used to introduce multiple functional groups into the shell of PDVB particles.[42] Other core-shell particles containing carbazole groups (fluorescence function) have been formed by distillation-precipitation polymerization.[44]

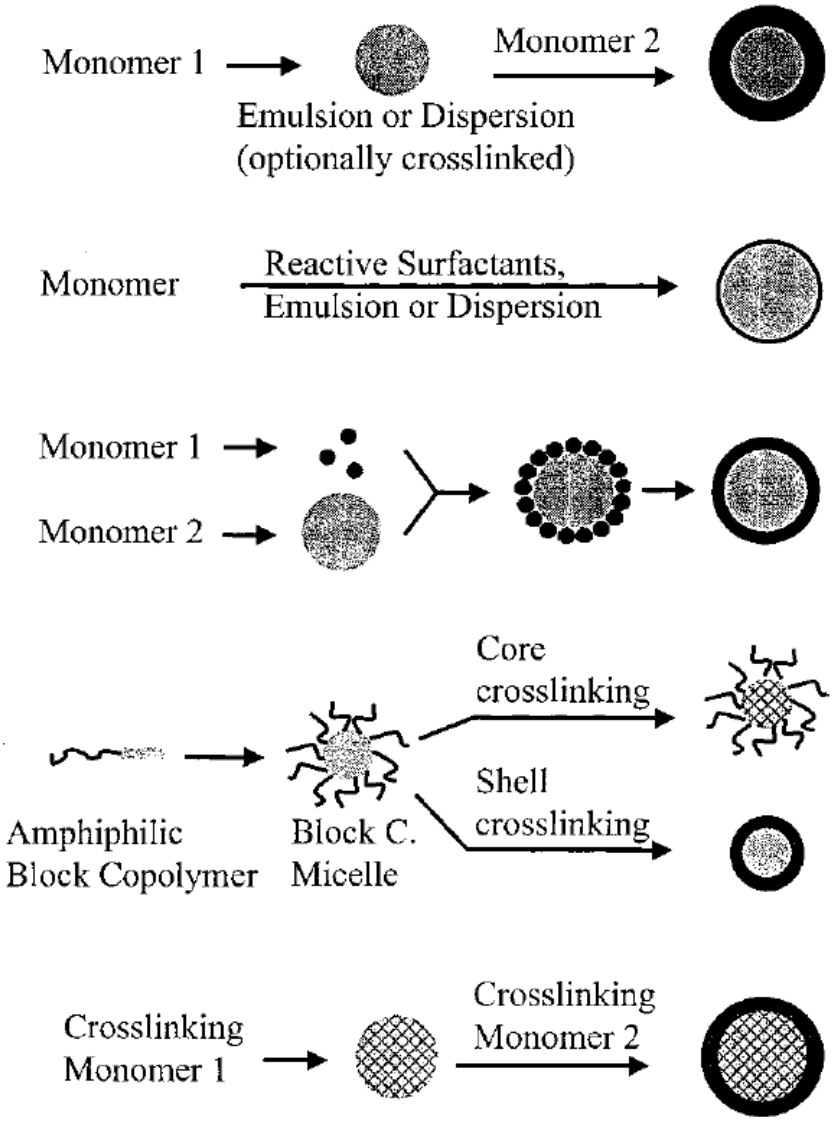

Scheme 1.3.5.1 Common approaches to core-shell particle[42] (Reprinted with permission from Ref.41, Copyright © 2000, American Chemical Society)

Among various types of polymer micro-particles, hollow particle is a unique type. For fabrication of such particles, a template is usually employed to form a core-shell structure first. The template core is sacrificed later by physical dissolution or chemical etching, while the shell remains. For instance, highly cross-linked PDVB/PEGMA hollow microspheres have been produced by distillation–precipitation.[45] Divinylbenzene (DVB) or ethylene glycol dimethacrylate

(EGDMA) is coated on the surface-modified silica template forming SiO_2–PDVB or SiO_2–PEGMA core–shell hybrid microspheres followed by removal of the silica core with hydrofluoric acid. This approach allows well-controlled particle size and designated shell thickness by carefully selecting template and grafting parameters.[45]

Double-shell PMAA–PNIPAM hollow microspheres were prepared by a combination of sol–gel chemistry and distillation–precipitation polymerization.[46] In this case, particles with poly(methacrylic acid) (PMAA) inner-shell and poly(N-isopropylacrylamide) (PNIPAM) outer-shell exhibited a unique hollow morphology that was pH and temperature responsive. Rattle-type particles consist of a movable core in a discrete shell. To access this morphology, core-shell seeds were prepared by distillation-precipitation polymerization, followed by another shell coating on the surface and removal of the middle layer.[45]

1.3.5.2 Chemical and thermal imprinting approaches

Based on precipitation polymerization, polymer microspheres with controlled core/shell structure can be produced in a single growth process via two approaches. One is chemical imprinting, where a second monomer is added during the polymerization to form microspheres containing a composite layer. In Cormack's work[47], precipitation polymerization was applied to fabricate imprinted spherical

particles in one single step. Theophylline-imprinted microspheres are prepared from PDVB/MAA particles with theophylline as comonomer.

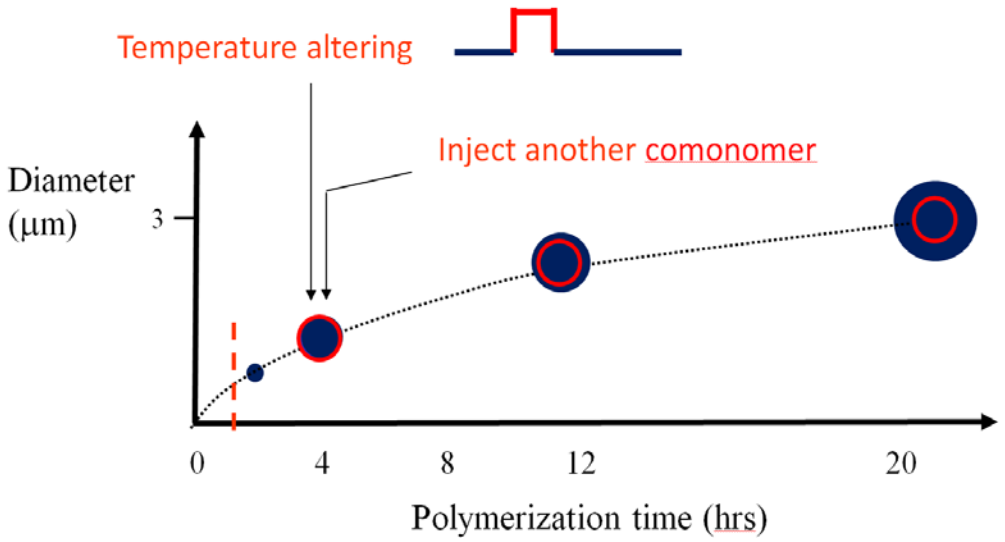

Scheme 1.3.5.2 Illustration of structured polymer microsphere

An alternative approach is thermal imprinting where the temperature is adjusted during the polymerization. An overall process of imprinting methodology is illustrated in Scheme 1.3.5.2, with the red ring representing either different composition or different density, corresponding to the chemical and thermal approaches, respectively. In our previous works by Takekoh and Stöver[48], polymer microspheres with multilayer patterns were fabricated by thermal imprinting during polymerization growth as shown in Figure 1.3.5.2.

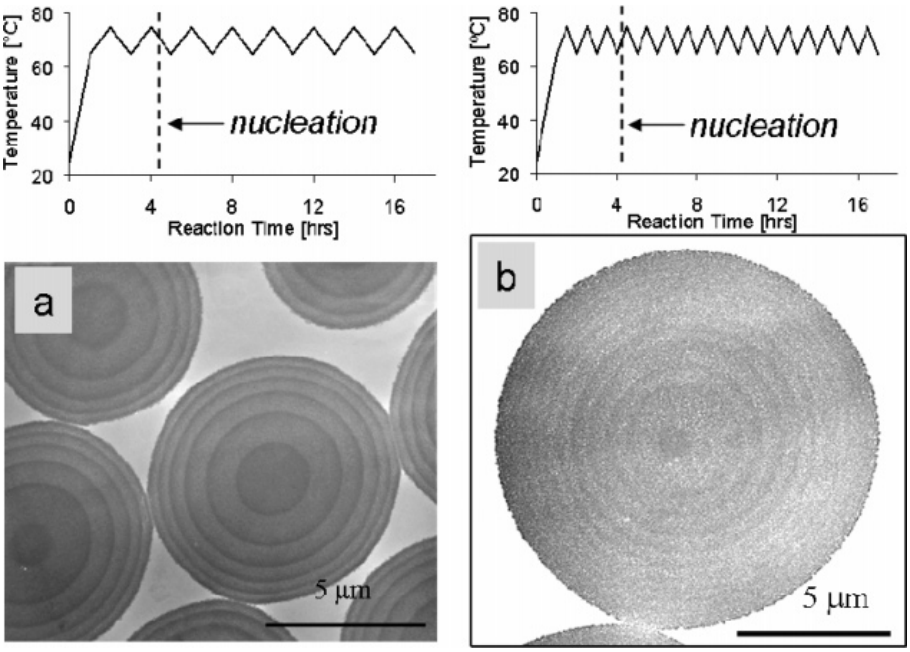

Figure 1.3.5.2 Transmission electronic microscopic images of onion particles with different thermal oscillation time[48] (Reprinted with permission from Ref.47, Copyright © 2005, American Chemical Society)

The onion-like microspheres consisting of layers with different density were synthesized by a one-pot process in this work. It shows precipitation copolymerization of DVB/CMS at low monomer loading (i.e. 2 vol.%) with effective cross-linker content (volume percent meta- and para-divinylbenzene in the total monomer pool) varying from 8 % to 11 % in acetonitrile. Particles grown with this composition proved sensitive to the thermal profile used. Growth-rings are imprinted into growing microspheres through thermal control of the surface gel layer during particle growth. As a result, 'zig-zag' temperature oscillations between 65^{o}C and 75^{o}C during particle growth become inscribed into the growing microspheres and remain visible after the polymerization. This process mimics the tree rings found in cross-sections of trees that reflect environmental conditions in

different seasons.

1.4 Potential Biomedical Application of Polymer Microspheres

Polymer microspheres have various applications, including as separation resins, drug delivery system and micro-reactors. Porous PDVB microspheres can be packed into columns for size exclusion chromatography[28]. In another research, chlorobenzyl particles were used as stationary phase in high-performance liquid chromatography.[49] Polymer particles have been investigated as drug-carriers in drug delivery systems. Ideally, the microsphere carriers can encapsulate active molecules, and can release them under external stimuli, such as pH changes.[50, 51] The most popular scenario is polymer particles that can retain drugs at physiological pH while facilitating drug release under mildly acidic conditions that is usually found for a variety of conditions, including tumors. Our group has interest in developing microspheres as potential cell scaffolds or as components of extracellular matrices (ECM).

1.4.1 Background of Extracellular Matrix

In vivo, cells are surrounded by a non-cellular component called extracellular matrix (ECM) that provides physical support and helps tissue morphogenesis, differentiation and homeostasis. ECM consists of water, proteins and

polysaccharides, which together form a three dimensional (3D) complex network, different in composition and topology for different tissues.[52] Far from an inert support, ECM has a highly dynamic structure, which influences the survival, development, migration, proliferation, shape and function of cells that are embedded.[53]

In contrast to cells *in vivo*, most *in vitro* cell studies are conducted on two dimensional (2D) cell cultures, with cells growing on top of the material surface. However, cell behaviors including adhesion, spreading, polarity and migration can show dramatic distinction between 2D and 3D contexts. The dissimilarity between these flat surfaces and 3D cellular microevironments *in vivo* limits our ability to model, and describe, native tissue functions.[54] For example, cells cultured on 2D supports have only part of the membranes in contact with ECM, which polarizes cells unnaturally.[55] The uncontacted parts of cells exposed to bulk culture media may experience homogenous soluble factors which are actually dynamic spatial gradients *in vivo*.[56] In certain cases, cells investigated in a 3D context provide insights that would never have been observed in traditional 2D systems, e.g. in terms of cell adhesion and structure,[57, 58] mechanotransduction,[59] and effector transport.[60] All these factors encourage development of 3D biomimetic cultures for studying fundamental cellular processes.[61]

1.4.2 Development of Materials

3D cell cultures have been long regarded as a fundamental research tool in cell biology with all the advantages discussed above. Over decades, ECM from natural sources, such as collagen[61], alginate[62] or fibrin[63], served as a useful platform. The limitation is the challenge in modifying specific factors independently without altering others. Synthetic hydrogels offer better control over composition, gelation conditions and allows final products with consistent properties. They can be tailored with specific biological, chemical and mechanical properties by controlling chemical composition, polymer concentration and molecular weight, as well as preparation methods. All these properties can influence behavior and function of cells, such as viability, differentiation and tissue formation.[64] Besides, synthesis of hydrogel can be conducted under mild conditions with properties easily adjusted by simple modifications.

Developing new materials then is required as one of the important goals for an understanding of how cells communicate with their surroundings and what the corresponding determinants are. For this specific application, polymer-based hydrogels are a promising candidate. Generally, hydrogels are water swellable and cross-linked polymer networks, possessing high permeability for small molecules, such as oxygen and nutrients. One example is poly(ethylene oxide)[65] as well as some of its copolymers, which have good cyto-compatibility. Ideally, hydrogels

combine the benefits of natural and synthetic materials, and show good potential to be used as scaffolds in 3D cell culture.[52]

1.4.3 Three Dimensional Polymer Scaffolds

1.4.3.1 Hydrogel beads

Cells can be encapsulated into polymer hydrogel beads, which offer attractive features. This strategy involves mixing cells and polymer precursors followed by gelation of the polymers. Cells are encapsulated during the polymer scaffold formation, either *in vitro* or *in vivo*. The scaffold can undergo designed degradation and meanwhile be gradually substituted by the newly developed ECM produced by cells, making the *in situ* repair of tissues feasible.[62] Such process requires good cyto- and host-compatibility, which must be considered in selecting candidate materials. Some preliminary work in cell encapsulation including biocompatible hydrogels from natural materials has been accomplished. Porous scaffolds were made from chitosan and natural polysaccharides with hydroxyl and amino groups[63], while further cell encapsulation works were focused on using synthetic hydrogels. For instance, poly(ethylene gylcol) (PEG) based hydrogels have been widely used for cell encapsulation.[64] Alginate-based hydrogel bead coated with poly-*l*-lysine and sodium alginate has also been systematically studied and Figure 1.4.2 shows the confocal images of alginate-based hydrogel beads recently

prepared.[65]

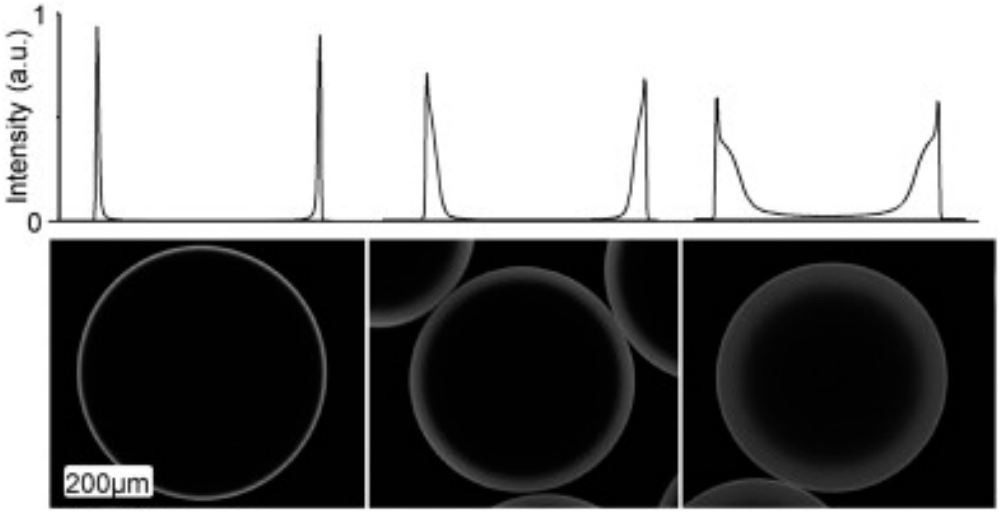

Figure 1.4.2 Line profiles (top) and equatorial confocal images (bottom) showing the distribution of PLL*f* in alginate/poly-L-lysine beads with different washing histories[65] (Reprinted with permission from Ref.47, Copyright © 2013 Published by Elsevier B.V.)

1.4.3.2 Hydrogel scaffolds

Synthetic hydrogels represent another class of materials for cell cultures.[66, 67] Many non-natural molecules have been employed for 3D gel formation. For examples, poly(ethylene glycol) based bulk hydrogels have been designed with oriented morphologies that can manipulate cell growth.[68] Poly(acrylamide) based hydrogel is another favored choice, with PNIPAM showing lower critical solution temperature (LCST) close to 37 ^{o}C, physiological temperature. PNIPAM-modified gelatins were photo-polymerized with different graft densities and molecular weight to form thermo-responsive 3D artificial scaffolds for cell proliferation.[69] Biocompatible and biodegradable poly(oxazoline) (POZ) is an alternative to PEG, with phase transition temperatures that can be varied by altering the co-monomer

ratio[70].

1.4.3.3 Porous scaffolds

Porous scaffolds, especially nanofibrous scaffolds, have drawn wide attention in tissue engineering because they can mimic the 3D architecture of ECM fibrillar proteins produced bycells. Several methods can be used for fabrication of porous scaffolds, such as electrospinning[71], solid free-form fabrication[72] or non-woven fiber mesh fabrication[73, 74]. Electrospinning is a widely adopted technique using an electrical jet of polymer solutions to produce various polymer fibers with diameter from nanometers to a few microns.[75, 76] The porosity of these polymer scaffolds provides high surface area for cell adhesion, proliferation and migration. The porous microstructure, however, makes it too fragile to handle the stress for proper mechanotransduction. Challenges remain with all these methods as sophisticated 3D environments are required for cell culture systems.

1.4.4 Particles Scaffolds

A new design of 3D cell scaffold was recently proposed based on polymer particles. By precipitation polymerization, the size of prepared microspheres can range from sub-micron to 15 micron. Both stiffness and porosity can be altered by adjusting the monomer loading and cross-linker content.[25, 39, 40] Also, inner structure and surface chemistry can be controlled by changing the monomer

compositions.[25, 27, 47, 77] Amphiphilic polymer particles, which consist of core-shell structures in some cases, allow a wide variety of pH- or temperature-responsive behaviors.[78-80] The great diversity in microsphere properties offers various strategies for optimizing scaffolds.

Polymer particles with diameter of about 100 micron have been fabricated by microfluidic method and applied as scaffolds for cell.[81] In this research, droplets containing methacrylated (MA) gelatin underwent photo-crosslinking process to generate particles, which were used as platform to proliferate cardiac cells for *in vitro* cell culture. In another work, the polymer scaffolds were fabricated based on photo-curable epoxy resin, a material which has been long regarded as a non-biocompatible material.[82] In that study, particles were fabricated with distinct micro-morphologies, while cells were cultured within the micro-wells formed by particle objects in arrays to pre-aggregate. As revealed by microscopic analysis, multiple cells were found to adhere to a single particle, while certain cells can line up and bridge a hole in an object, suggesting a great diversity in micro-interactions between cells and polymer objects.

Besides, the gel layer intermediate during particle formation in precipitation polymerization can undergo functionalization to meet diverse applicability. For traditional scaffolds, properties are set once the particle is formed, leaving little modification ability for post-treatment. Comparatively, the functional group, such as

chlorine on particles surface in DVB/CMS microspheres system, provides great potential for further functionalization, reasonably incorporated with biomimetic signals. For example, hydrophilic microspheres with reactive chloroalkyl groups were successfully fabricated, offering several functionalization possibilities.[83] Particle hydrophobicity / hydrophilicity levels can be well adjusted by hydrophilization of functional groups, which has been reviewed before.[84]

1.5 Thesis Objectives

The overall objective of this thesis work is the fabrication and investigation of polymer microspheres by thermal imprinting precipitation polymerization. Precipitation polymerization is a unique method for the fabrication of mono-disperse microspheres with clean surfaces, and has recently been used to form core-shell and hollow microspheres.

In my research, thermal imprinting is applied to develop internally structured poly(CMS-*co*-DVB) microspheres. Objectives include understanding of radial structuring of precipitation polymer particles through thermal means, network formation and *theta* conditions. Future work may include generalizing thermal imprinting from current system to more hydrophilic comonomer systems.

Hydrophilic microspheres are of great interests as our ultimate target is to explore hydrophilic microspheres as a component of extracellular matrix and tissue scaffolds. Future work in this direction may include:

- Preparing and charactering hydrophilic microspheres by surface modification of poly(CMS-*co*-DVB) hydrophobic microspheres;
- Preparing and charactering hydrophilic microspheres from DVB/MAn system followed by hydrolysis;
- Studying interaction between cells and particles.

1.6 Reference

1. Winslow, F.H. and W. Matreyek, *Particle Size in Suspension Polymerization.* Industrial & Engineering Chemistry, 1951. **43**(5): p. 1108-1112.
2. Arshady, R., *Suspension, emulsion, and dispersion polymerization: A methodological survey.* Colloid and Polymer Science, 1992. **270**(8): p. 717-732.
3. Arshady, R. and A. Ledwith, *Suspension polymerisation and its application to the preparation of polymer supports.* Reactive Polymers, Ion Exchangers, Sorbents, 1983. **1**(3): p. 159-174.
4. Balakrishnan, T. and W.T. Ford, *Particle size control in suspension copolymerization of styrene, chloromethylstyrene, and divinylbenzene.* Journal of Applied Polymer Science, 1982. **27**(1): p. 133-138.
5. Macintyre, F.S. and D.C. Sherrington, *Control of Porous Morphology in Suspension Polymerized Poly(divinylbenzene) Resins Using Oligomeric Porogens.* Macromolecules, 2004. **37**(20): p. 7628-7636.
6. Howard, G.J. and C.A. Midgley, *The formation and structure of suspension-polymerized styrene–divinylbenzene copolymers.* Journal of Applied Polymer Science, 1981. **26**(11): p. 3845-3870.
7. Dowding, P.J. and B. Vincent, *Suspension polymerisation to form polymer beads.* Colloids and Surfaces A: Physicochemical and Engineering Aspects, 2000. **161**(2): p. 259-269.
8. Jonsson, M., et al., *Suspension polymerization of thermally expandable core/shell particles.* Polymer, 2006. **47**(10): p. 3315-3324.
9. Okubo, M., Y. Konishi, and H. Minami, *Production of hollow polymer particles by suspension polymerizations for divinylbenzene/toluene droplets dissolving various polymers.* Colloid and Polymer Science, 2000. **278**(7): p. 659-664.
10. *emulsion polymerization*. Art [cited 2015 03/22]; Available from: http://kids.britannica.com/elementary/art-121408.

11. Chern, C.S., *Emulsion polymerization mechanisms and kinetics.* Progress in Polymer Science, 2006. **31**(5): p. 443-486.
12. Gardon, J.L., *Emulsion polymerization. II. Review of experimental data in the context of the revised Smith-Ewart theory.* Journal of Polymer Science Part A-1: Polymer Chemistry, 1968. **6**(3): p. 643-664.
13. Israelachvili, J.N., *Intermolecular and surface forces: revised third edition*. 2011: Academic press.
14. Juang, M.S.-D. and I.M. Krieger, *Emulsifier-free emulsion polymerization with ionic comonomer.* Journal of Polymer Science: Polymer Chemistry Edition, 1976. **14**(9): p. 2089-2107.
15. Goodall, A.R., M.C. Wilkinson, and J. Hearn, *Mechanism of emulsion polymerization of styrene in soap-free systems.* Journal of Polymer Science: Polymer Chemistry Edition, 1977. **15**(9): p. 2193-2218.
16. Lok, K.P. and C.K. Ober, *Particle size control in dispersion polymerization of polystyrene.* Canadian Journal of Chemistry, 1985. **63**(1): p. 209-216.
17. Paine, A.J., *Dispersion polymerization of styrene in polar solvents. IV. Solvency control of particle size from hydroxypropyl cellulose stabilized polymerizations.* Journal of Polymer Science Part A: Polymer Chemistry, 1990. **28**(9): p. 2485-2500.
18. Bamnolker, H. and S. Margel, *Dispersion polymerization of styrene in polar solvents: effect of reaction parameters on microsphere surface composition and surface properties, size and size distribution, and molecular weight.* Journal of Polymer Science Part A: Polymer Chemistry, 1996. **34**(10): p. 1857-1871.
19. Paine, A.J., W. Luymes, and J. McNulty, *Dispersion polymerization of styrene in polar solvents. 6. Influence of reaction parameters on particle size and molecular weight in poly (N-vinylpyrrolidone)-stabilized reactions.* Macromolecules, 1990. **23**(12): p. 3104-3109.
20. Li, G.L., H. Möhwald, and D.G. Shchukin, *Precipitation polymerization for fabrication of complex core–shell hybrid particles and hollow structures.* Chemical Society Reviews, 2013. **42**(8): p. 3628-3646.
21. Li, K. and H.D. Stöver, *Synthesis of monodisperse poly (divinylbenzene) microspheres.* Journal of Polymer Science Part A: Polymer Chemistry, 1993. **31**(13): p. 3257-3263.
22. Romack, T.J., E.E. Maury, and J.M. DeSimone, *Precipitation Polymerization of Acrylic Acid in Supercritical Carbon Dioxide.* Macromolecules, 1995. **28**(4): p. 912-915.
23. Laska, J., J. Widlarz, and E. Woźny, *Precipitation polymerization of aniline in the presence of water-soluble organic acids.* Journal of Polymer Science Part A: Polymer Chemistry, 2002. **40**(21): p. 3562-3569.

24. Liu, T., et al., *Particle Formation in Precipitation Polymerization: Continuous Precipitation Polymerization of Acrylic Acid in Supercritical Carbon Dioxide.* Macromolecules, 2006. **39**(19): p. 6489-6494.
25. Frank, R.S., J.S. Downey, and H. Stöver, *Synthesis of divinylbenzene–maleic anhydride microspheres using precipitation polymerization.* Journal of Polymer Science Part A: Polymer Chemistry, 1998. **36**(13): p. 2223-2227.
26. Frank, R.S., et al., *Poly (divinylbenzene-alt-maleic anhydride) microgels: intermediates to microspheres and macrogels in cross-linking copolymerization.* Macromolecules, 2002. **35**(7): p. 2728-2735.
27. Li, W.H., K. Li, and H.D. Stöver, *Monodisperse poly (chloromethylstyrene-co-divinylbenzene) microspheres by precipitation polymerization.* Journal of Polymer Science Part A: Polymer Chemistry, 1999. **37**(14): p. 2295-2303.
28. Li, W.H. and H.D. Stöver, *Porous monodisperse poly (divinylbenzene) microspheres by precipitation polymerization.* Journal of Polymer Science Part A: Polymer Chemistry, 1998. **36**(10): p. 1543-1551.
29. Bai, F., X. Yang, and W. Huang, *Synthesis of narrow or monodisperse poly (divinylbenzene) microspheres by distillation-precipitation polymerization.* Macromolecules, 2004. **37**(26): p. 9746-9752.
30. Bai, F., X. Yang, and W. Huang, *Preparation of narrow or monodisperse poly (ethyleneglycol dimethacrylate) microspheres by distillation–precipitation polymerization.* European polymer journal, 2006. **42**(9): p. 2088-2097.
31. Bai, F., et al., *Monodisperse hydrophilic polymer microspheres having carboxylic acid groups prepared by distillation precipitation polymerization.* Polymer, 2006. **47**(16): p. 5775-5784.
32. Bai, F., et al., *Preparation of narrow-dispersion or monodisperse polymer microspheres with active hydroxyl group by distillation–precipitation polymerization.* Polymer international, 2006. **55**(3): p. 319-325.
33. Bai, F., et al., *Synthesis of monodisperse poly (methacrylic acid) microspheres by distillation–precipitation polymerization.* European Polymer Journal, 2007. **43**(9): p. 3923-3932.
34. Limé, F. and K. Irgum, *Monodisperse polymeric particles by photoinitiated precipitation polymerization.* Macromolecules, 2007. **40**(6): p. 1962-1968.
35. Joso, R., et al., *Ambient temperature synthesis of well-defined microspheres via precipitation polymerization initiated by UV-irradiation.* Journal of Polymer Science Part A: Polymer Chemistry, 2007. **45**(15): p. 3482-3487.
36. Lime, F. and K. Irgum, *Preparation of divinylbenzene and divinylbenzene-co-glycidyl methacrylate particles by photoinitiated precipitation polymerization in different solvent mixtures.* Macromolecules, 2009. **42**(13): p. 4436-4442.
37. Zheng, G. and H.D. Stöver, *Grafting of polystyrene from narrow disperse*

polymer particles by surface-initiated atom transfer radical polymerization. Macromolecules, 2002. **35**(18): p. 6828-6834.

38. Zheng, G. and H.D. Stöver, *Grafting of poly (alkyl (meth) acrylates) from swellable poly (DVB80-co-HEMA) microspheres by atom transfer radical polymerization.* Macromolecules, 2002. **35**(20): p. 7612-7619.
39. Downey, J.S., et al., *Poly (divinylbenzene) microspheres as an intermediate morphology between microgel, macrogel, and coagulum in cross-linking precipitation polymerization.* Macromolecules, 2001. **34**(13): p. 4534-4541.
40. Downey, J.S., et al., *Growth mechanism of poly (divinylbenzene) microspheres in precipitation polymerization.* Macromolecules, 1999. **32**(9): p. 2838-2844.
41. Medina-Castillo, A.L., et al., *Micrometer and Submicrometer Particles Prepared by Precipitation Polymerization: Thermodynamic Model and Experimental Evidence of the Relation between Flory's Parameter and Particle Size.* Macromolecules, 2010. **43**(13): p. 5804-5813.
42. Li, W.-H. and H.D. Stöver, *Monodisperse cross-linked core-shell polymer microspheres by precipitation polymerization.* Macromolecules, 2000. **33**(12): p. 4354-4360.
43. Tanaka, T., N. Saito, and M. Okubo, *Control of Layer Thickness of Onionlike Multilayered Composite Polymer Particles Prepared by the Solvent Evaporation Method†.* Macromolecules, 2009. **42**(19): p. 7423-7429.
44. Qi, D., X. Yang, and W. Huang, *Preparation of monodisperse fluorescent core–shell polymer microspheres with functional groups in the shell layer by two-stage distillation–precipitation polymerization.* Polymer international, 2007. **56**(2): p. 208-213.
45. Li, G. and X. Yang, *Facile synthesis of hollow polymer microspheres with movable cores with the aid of hydrogen-bonding interaction.* The Journal of Physical Chemistry B, 2007. **111**(44): p. 12781-12786.
46. Li, G., et al., *Narrowly dispersed double-walled concentric hollow polymeric microspheres with independent pH and temperature sensitivity.* Macromolecules, 2008. **41**(23): p. 9487-9490.
47. Wang, J., et al., *Monodisperse, Molecularly Imprinted Polymer Microspheres Prepared by Precipitation Polymerization for Affinity Separation Applications.* Angewandte Chemie International Edition, 2003. **42**(43): p. 5336-5338.
48. Takekoh, R., et al., *Multilayered polymer microspheres by thermal imprinting during microsphere growth.* Journal of the American Chemical Society, 2006. **128**(1): p. 240-244.
49. Perrier-Cornet, R., et al., *Functional crosslinked polymer particles synthesized by precipitation polymerization for liquid chromatography.*

Journal of Chromatography A, 2008. **1179**(1): p. 2-8.

50. Skirtach, A.G., A.M. Yashchenok, and H. Mohwald, *Encapsulation, release and applications of LbL polyelectrolyte multilayer capsules.* Chemical Communications, 2011. **47**(48): p. 12736-12746.
51. Rosenbauer, E.-M., et al., *Controlled Release from Polyurethane Nanocapsules via pH-, UV-Light- or Temperature-Induced Stimuli.* Macromolecules, 2010. **43**(11): p. 5083-5093.
52. Frantz, C., K.M. Stewart, and V.M. Weaver, *The extracellular matrix at a glance.* Journal of cell science, 2010. **123**(24): p. 4195-4200.
53. Tibbitt, M.W. and K.S. Anseth, *Hydrogels as extracellular matrix mimics for 3D cell culture.* Biotechnology and Bioengineering, 2009. **103**(4): p. 655-663.
54. Baker, B.M. and C.S. Chen, *Deconstructing the third dimension–how 3D culture microenvironments alter cellular cues.* Journal of cell science, 2012. **125**(13): p. 3015-3024.
55. Zhang, S., X. Zhao, and L. Spirio, *PuraMatrix: self-assembling peptide nanofiber scaffolds.* Scaffolding in tissue engineering, 2005: p. 217-238.
56. Ashe, H.L. and J. Briscoe, *The interpretation of morphogen gradients.* Development, 2006. **133**(3): p. 385-394.
57. Mseka, T., J.R. Bamburg, and L.P. Cramer, *ADF/cofilin family proteins control formation of oriented actin-filament bundles in the cell body to trigger fibroblast polarization.* Journal of cell science, 2007. **120**(24): p. 4332-4344.
58. Khetan, S. and J.A. Burdick, *Patterning network structure to spatially control cellular remodeling and stem cell fate within 3-dimensional hydrogels.* Biomaterials, 2010. **31**(32): p. 8228-8234.
59. Huebsch, N., et al., *Harnessing traction-mediated manipulation of the cell/matrix interface to control stem-cell fate.* Nat Mater, 2010. **9**(6): p. 518-526.
60. Volkmer, E., et al., *Hypoxia in static and dynamic 3D culture systems for tissue engineering of bone.* Tissue Engineering Part A, 2008. **14**(8): p. 1331-1340.
61. Pampaloni, F., E.G. Reynaud, and E.H.K. Stelzer, *The third dimension bridges the gap between cell culture and live tissue.* Nat Rev Mol Cell Biol, 2007. **8**(10): p. 839-845.
62. Nicodemus, G.D. and S.J. Bryant, *Cell encapsulation in biodegradable hydrogels for tissue engineering applications.* Tissue Engineering Part B: Reviews, 2008. **14**(2): p. 149-165.
63. Madihally, S.V. and H.W.T. Matthew, *Porous chitosan scaffolds for tissue engineering.* Biomaterials, 1999. **20**(12): p. 1133-1142.
64. Koh, W.-G., A. Revzin, and M.V. Pishko, *Poly(ethylene glycol) Hydrogel Microstructures Encapsulating Living Cells.* Langmuir, 2002. **18**(7): p. 2459-

2462.

65. Kleinberger, R.M., et al., *Systematic study of alginate-based microcapsules by micropipette aspiration and confocal fluorescence microscopy.* Materials Science and Engineering: C, 2013. **33**(7): p. 4295-4304.
66. Saha, K., et al., *Designing synthetic materials to control stem cell phenotype.* Current opinion in chemical biology, 2007. **11**(4): p. 381-387.
67. Lutolf, M., et al., *Synthetic matrix metalloproteinase-sensitive hydrogels for the conduction of tissue regeneration: engineering cell-invasion characteristics.* Proceedings of the National Academy of Sciences, 2003. **100**(9): p. 5413-5418.
68. Schulte, V.A., et al., *Microengineered PEG hydrogels: 3D scaffolds for guided cell growth.* Macromolecular bioscience, 2013. **13**(5): p. 562-572.
69. Ohya, S. and T. Matsuda, *Poly (N-isopropylacrylamide)(PNIPAM)-grafted gelatin as thermoresponsive three-dimensional artificial extracellular matrix: molecular and formulation parameters vs. cell proliferation potential.* Journal of Biomaterials Science, Polymer Edition, 2005. **16**(7): p. 809-827.
70. Wang, X., et al., *Synthesis, characterization and biocompatibility of poly(2-ethyl-2-oxazoline)–poly(d,l-lactide)–poly(2-ethyl-2-oxazoline) hydrogels.* Acta Biomaterialia, 2011. **7**(12): p. 4149-4159.
71. Barnes, C.P., et al., *Nanofiber technology: Designing the next generation of tissue engineering scaffolds.* Advanced Drug Delivery Reviews, 2007. **59**(14): p. 1413-1433.
72. Giordano, R.A., et al., *Mechanical properties of dense polylactic acid structures fabricated by three dimensional printing.* Journal of Biomaterials Science, Polymer Edition, 1997. **8**(1): p. 63-75.
73. Freed, L.E., et al., *Biodegradable Polymer Scaffolds for Tissue Engineering.* Nat Biotech, 1994. **12**(7): p. 689-693.
74. Hutmacher, D.W., *Scaffold design and fabrication technologies for engineering tissues — state of the art and future perspectives.* Journal of Biomaterials Science, Polymer Edition, 2001. **12**(1): p. 107-124.
75. *Electrospun silk fibroin tubular matrixes for small vessel bypass grafting.* Materials Technology, 2009. **24**(1): p. 52-57.
76. Yoshimoto, H., et al., *A biodegradable nanofiber scaffold by electrospinning and its potential for bone tissue engineering.* Biomaterials, 2003. **24**(12): p. 2077-2082.
77. Li, W.H. and H.D. Stöver, *Mono-or narrow disperse poly (methacrylate-co-divinylbenzene) microspheres by precipitation polymerization.* Journal of Polymer Science Part A: Polymer Chemistry, 1999. **37**(15): p. 2899-2907.
78. Fleischmann, C., et al., *A robust platform for functional microgels via thiol-ene chemistry with reactive polyether-based nanoparticles.* Polymer

Chemistry, 2015.

79. Ho, K., et al., *Amphiphilic polymeric particles with core–shell nanostructures: emulsion-based syntheses and potential applications.* Colloid and Polymer Science, 2010. **288**(16-17): p. 1503-1523.
80. Bernards, M. and Y. He, *Polyampholyte polymers as a versatile zwitterionic biomaterial platform.* Journal of Biomaterials Science, Polymer Edition, 2014. **25**(14-15): p. 1479-1488.
81. Cha, C., et al., *Microfluidics-Assisted Fabrication of Gelatin-Silica Core–Shell Microgels for Injectable Tissue Constructs.* Biomacromolecules, 2014. **15**(1): p. 283-290.
82. Leferink, A., et al., *Engineered Micro-Objects as Scaffolding Elements in Cellular Building Blocks for Bottom-Up Tissue Engineering Approaches.* Advanced materials, 2014. **26**(16): p. 2592-2599.
83. Kip, Ç., et al., *A new type of monodisperse porous, hydrophilic microspheres with reactive chloroalkyl functionality: synthesis and derivatization properties.* Colloid and Polymer Science, 2014. **292**(1): p. 219-228.
84. Oh, S.H. and J.H. Lee, *Hydrophilization of synthetic biodegradable polymer scaffolds for improved cell/tissue compatibility.* Biomedical Materials, 2013. **8**(1): p. 014101.

CHAPTER TWO

2 Structured Poly(divinylbenzene-*co*-chloromethylstyrene) Microspheres by Thermal Imprinting Precipitation Polymerization

Zhao, Yuqing; Burke, Nicholas A.D.; Stöver, Harald D.H.

Department of Chemistry and Chemical Biology

McMaster University, 1280 Main Street W, Hamilton, ON, Canada

Note: The work described in this chapter was carried out by Yuqing Zhao. This chapter was written by Yuqing Zhao, with editing provided by N. Burke and H Stöver. N. Burke and H. Stöver also provided guidance during the course of the work. This chapter is to be published in J. Polym. Sci. Polym. Chem.

2.1 Abstract

The free radical precipitation copolymerization of chloromethylstyrene and divinylbenzene in acetonitrile is reported, leading to mono-disperse, crosslinked microspheres with radial density profiles in good solvents that match the thermal profiles used during copolymerization. Stepping down the polymerization temperature from 75 °C to 65 °C several hours into the copolymerization led to core-shell microspheres with porous cores and denser shells, while stepping up the

polymerization temperature from 68 °C to 78 °C during the polymerization led to formation of microspheres with denser cores and more swellable shells.

Microsphere size distributions and internal morphologies were studied using optical and transmission electron microscopy. The change in network swellability with temperature was compared with model studies of aggregation of corresponding oligomers in acetonitrile and similar solvent systems as a function of temperature, indicating the *theta*-temperature for this copolymer / solvent system to be around 30 °C.

2.2 Introduction

Precipitation polymerization is a method uniquely suited to the formation of mono-disperse, crosslinked microspheres with clean surfaces. It typically involves free radical polymerization of vinyl monomers using thermal,[1, 2] or photo-initiators,[3] often in the presence of crosslinking comonomers. The choice of solvent is critical, as polymer-solvent interactions govern the aggregation of initially formed oligomers into particle nuclei, while providing colloidal stability to the resulting, growing polymer particles. Successful precipitation polymerizations comprise an initial, limited particle nucleation period, followed by particle growth through capturing of further oligomers and monomers. Colloidal stability during particle growth is provided by the continuously renewing thin gel/oligomer layer

present on the particle surface.[4]

Originally developed for polymerization of divinylbenzene-55 (DVB55)[1], and subsequently for copolymerization of chloromethylstyrene,[5] maleic anhydride,[6, 7] or methacrylic monomers[8] with DVB55 or ethylenedimethacrylate (EDMA) in acetonitrile and MEK/Heptane mixtures, the method has since been expanded to include, i.e., photo-initiation,[3] distillation-precipitation polymerization, and controlled radical polymerization.[9] Bai et al. showed that covalent crosslinking can be replaced by hydrogen-bonding interactions between acrylic acid units, allowing the formation of polyacrylic acid microspheres,[10] and acetic acid can be used as solvent instead of acetonitrile.[11] Matching Hansen solubility parameters of polymer and solvent(s) proved useful in precipitation copolymerizations of polar comonomers including EDMA, methacrylic acid and PEG methacrylate.[12]

The radial growth process together with the presence of residual vinyl groups on surfaces of the resulting particles have been used for post-modifications by grafting using ATRP[13] and RAFT[14], as well as for formation of distinct shells through a second stage of precipitation polymerization in presence of porogens or additional comonomers.[4, 15] Yang used distillation–precipitation polymerization to form PMAA cores held together by hydrogen-bonding crosslinking, coated these with PDVB shells and then extracted the PMAA core under basic conditions to form hollow shells.[16] Two recent reviews cover microspheres with complex internal

structures prepared by precipitation polymerization.[17, 18]

An alternative, less explored approach to core-shell microspheres by precipitation polymerization is based on the thermal responsiveness of the lightly crosslinked surface gel layer during growth phase. We showed recently that moderate thermal oscillations during batch-precipitation polymerizations can be used to inscribe corresponding concentric layers of different swellability into certain microspheres.[19] These microspheres were formed by free-radical precipitation copolymerization of DVB55 and chloromethylstyrene (CMS) in acetonitrile, at DVB55/CMS ratios of about 1:5, corresponding to molar ratios of m/p-divinylbenzene / monovinyl species, called effective crosslinker ratios, of 8-10 %.

The current paper explores this thermal imprinting process in more detail, and in part as a step towards extending this approach to other comonomer systems. To this end we used step-up and step-down thermal profiles to explore the formation of dense core – swollen shell, and swollen core – dense shell structures, respectively. Optical and transmission electron microscopy were used to compare microsphere sizes and internal structures with thermal profiles. In addition, we explored the solvation as a function of temperature for model copolymer nanogels, in both acetonitrile (a marginal solvent for styrenic polymers) and in mixtures of acetonitrile with good and poor co-solvents, to develop tools for extending this concept of thermal imprinting to other comonomer systems.

2.3 Experimental

2.3.1 Materials

Commercial divinylbenzene-55 (DVB-55, 55 % divinylbenzene isomers, 45 % ethylstyrene isomers, Sigma-Aldrich), chloromethylstyrene (CMS, mixture of 3- and 4-isomers, Aldrich Chem. Inc.), solvents (acetonitrile, HPLC grade, Caledon Labs; methanol, HPLC grade, Caledon Labs; xylenes, certified A.C.S., Fisher Scientific; $CDCl_3$, Cambridge Isotope Laboratories. Inc.) were used as received. Initiator (2,2'-azobis(2-methylpropionitrile) (AIBN, Dupont) was recrystallized from methanol. Commercial Spurr's embedding resin (Polysciences, Inc.) was used for TEM embedding according to the following recipe: dry microspheres were placed in the tips of polypropylene bullet cases, followed by the just-mixed resin, and cured for 12 hrs at 70 °C temperature. Sections were prepared by ultra-microtoming to 100 nm using a diamond knife.

2.3.2 Preparation of microspheres

Following an earlier procedure,[20] DVB-55 and CMS were added to neat acetonitrile to give 20.0 mL of solutions containing 2, 3, or 4 vol.% total monomer, of which 8, 5.3 or 4 vol.% were actual crosslinker (3- or 4-divinylbenzene) relative to total monomer. AIBN initiator was added at 2 wt % relative to total monomers.

For example, for a polymerization with 2 vol.% total monomer loading and 8 % effective cross-linker, 0.058 mL (0.053 g) DVB-55, 0.342 mL (0.367 g) CMS and 0.0084 g AIBN were dissolved in 19.6 mL acetonitrile in a 25 mL glass screw cap vial. These vials were placed in an oven fitted with a programmable thermostat and a set of steel rollers rotating at 4 rpm. Polymerizations were carried out at constant temperatures, or using thermal profiles as described in Fig. 1 below. The rate of temperature change for both step-up and step-down was measured using a small thermometer inserted in a reaction vial filled with 20 mL water, and indicated that the temperature changes were complete to within 1 °C in 30 minutes. This represents an upper limit, given the higher heat capacity of water compared to acetonitrile. The composition of the resulting microspheres was described as, e.g., 2E8 for 2 % total monomer loading of which 8 % was effective crosslinker (m/p-divinylbenzene). The thermal profiles were encoded in the name as described in the results section.

At the end of the reactions, the vials were opened briefly to terminate the polymerization and then allowed to cool to room temperature. The reaction mixtures were allowed to settle overnight and the supernatant was removed. The microspheres were re-suspended in xylenes for characterization by optical microscopy, and for embedding in Spurr’s resin and characterization by TEM. Typical yields of isolated microspheres ranged from 5 to 15 %.

2.3.3 Preparation of Poly(DVB-*co*-CMS) Model Nanogels

Polymerizations were carried out as described for the microspheres above, except that compositions were limited to 2 vol.% total monomer, comprising 8 vol.% m/p-divinylbenzene. Reactions were carried out at 70 °C, vials were removed after 2, 3 and 4 hrs, opened briefly to stop the polymerization, and the resulting reaction mixture precipitated into seven-fold excess HPLC grade methanol. The solid nanogels were isolated by centrifugation, the supernatant removed and the nanogels washed with methanol three times. Finally, all samples were dried under vacuum overnight at room temperature. About 20–50 mg of solid was isolated for each sample. The resulting samples are called 2E8 (70) 2h, 2E8 (70) 3h, and 2E8 (70) 4h.

2.3.4 Characterization

2.3.4.1 Optical microscopy

The diameters of dry and xylene-swollen copolymer microspheres were determined from images obtained with an Olympus BX51 optical microscope in transmission mode. Typically 100 microspheres were measured for each sample, using Image Pro software. Particles were allowed to swell in xylenes for 5 minutes prior to measurements.

2.3.4.2 Transmission electron microscopy

The internal structure of the microspheres was obtained using a JEOL 1200EX TEMSCAN transmission electron microscope (TEM). The TEM samples were prepared by embedding microspheres in Spurr's resin. To prepare the resin, 10 g vinylcyclohexene dioxide, 26 g nonenyl succinic anhydride, 6 g diglycidyl ether of polypropyleneglycol, and 0.4 g dimethylaminoethanol were mixed, and used to embed the xylene swollen microspheres in polypropylene bullet moulds, curing at 70 °C overnight. Embedded samples were ultra-microtomed to about 100 nm thick sections and deposited on 3 mm copper/platinum TEM grids. All TEM images shown here have their brightness increased by 20 %, compared to the original digital images. Microsphere samples were typically narrow-disperse, though TEM images show different apparent diameters due to random vertical position relative to the sectioning plane. The images shown are representative of the respective samples. Equatorial sections with the largest diameter were used to determine core and shell diameters.

2.3.4.3 Proton NMR

Proton NMR analysis was performed using a Bruker AV 600 spectrometer. Approximately 10 mg oligomer was dispersed in 1 mL of $CDCl_3$ and 64 scans were performed for each sample and 5 Hz line broadening was applied to the oligomer/microsphere spectra. The conversion of vinyl groups was calculated from the relative integral of the vinyl group on divinylbenzene (1H for each peak, around

5.6 to 6.5 ppm) to methylene group on chloromethylstyrene (2H, 4.49 ppm).

2.3.4.4 Turbidimetry

Turbidity measurements were conducted on a Varian Cary 3E spectrophotometer fitted with a temperature controlled 12-sample cell holder. About 1.2 mg of each nanogel sample were dispersed in 3 mL of neat acetonitrile, acetonitrile with 2 vol.% xylene, or acetonitrile with 5 vol.% methanol, respectively. This corresponds to a concentration of nanogel that is about 2 to 3 times lower than that in native polymerizations at 2-3 hours polymerization. The dispersions were turbid at room temperature but became clear upon heating to 65 °C. Transmissivity was measured at a wavelength of 500 nm during cooling from 65 °C to 15 °C at 1 °C/min, with data points collected every 0.5 °C. The resulting curves were normalized to 100 % transmissivity at high temperature in order to eliminate small differences due to the glass cuvettes being used for these experiments.

2.4 Results and Discussion

2.4.1 Thermal profile

We previously noticed that cycling the polymerization temperature during precipitation copolymerizations of DVB55 with CMS in acetonitrile between 65 °C and 75 °C led to the appearance of corresponding concentric growth rings in the final particles.[19] These concentric layers have differential swellabilities in good

solvents, caused by temperature-dependent crosslinking efficiencies imprinted during particle growth. They are visible by optical and transmission electron microscopy, when swollen in good solvents such as xylene or Spurr's resin, respectively.

This phenomenon was attributed to the significant thermal chain expansion of DVB55/CMS oligomers in acetonitrile at these temperatures. Specifically, there appears to be sufficient polymer-solvent affinity at 65 °C to maintain colloidal stability during growth through steric stabilization by the transient surface gel layer, while increasing the temperature to 78 °C resulted in deposition of correspondingly more swollen oligomers.

The present work explores the potential of this thermal imprinting approach to form hollow capsules and dense core/swellable shell particles. The step-down profile led to capsule-like microspheres with swellable cores and denser shells, while the step-up profiles led to microspheres with denser cores and swellable shells. At the same time we aim to develop conceptual and experimental tools for extending this approach to other monomer/solvent combinations. Polymerizations were carried out using the step-up and step-down profiles as shown in Figure 1 as well as at constant temperatures of 68 °C and 75 °C.

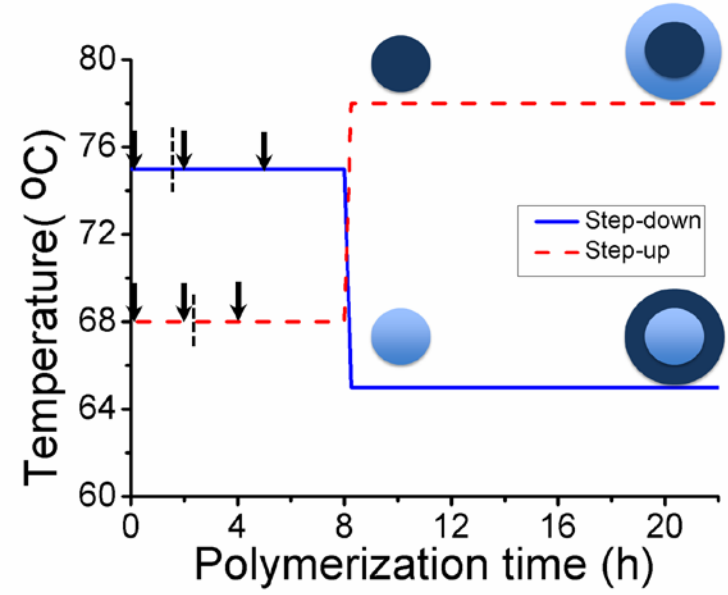

Figure 1. Temperature profiles of step-down (blue line), step-up process (red line). The downward-pointing arrows denote the time reaction vials were placed in the polymerization reactor. The vertical dashed lines indicate approximate particle nucleation times (appearance of turbidity) at high and low temperatures, for reaction vials added at t = 0 hrs. The structures shown are meant to illustrate the internal morphologies seen upon swelling in good solvents.

For the step-up profile, the polymerization reactor temperature was stabilized at 68 °C, sample vials were added at t = 0, 2 and 4 hrs (vertical arrows) and reacted at this temperature for, respectively, 8, 6 and 4 hrs. At t = 8 hrs, the temperature was rapidly increased to 78 °C and held there until t = 22 hrs. For the step-down profile, the reactor temperature was stabilized at 75 °C, sample vials were added at t = 0, 2 and 5 h and polymerized at this temperature for, respectively, 8, 6 and 3 h. At t = 8 hrs the temperature was rapidly decreased to 65 °C and the reaction continued until t = 22 hrs. The 3 h initial plateau time for this profile was chosen because of the higher polymerization rate at this temperature.

A step-down profile starting with a 78 °C segment was explored initially, but was found to lead to polydispersed particles, possibly due to extended nucleation at this combination of high temperature and high monomer loading. The temperature of the initial segment was then adjusted to 75 °C and narrow disperse particles were observed.

Codes such as **2E8/t** and **2E8\t** are used to describe both total monomer loading (**2** vol.%), effective crosslinker *m*/*p*-divinylbenzene (**E8**), and thermal profile (**/t** = step-up from 68 °C to 78 °C at **t** hrs, followed by **14** hrs at 78 °C; **\t** = step-down from 75 °C to 65 °C at **t** hrs, followed by **14** hrs at 65 °C). The polymerizations at constant temperatures of 68 °C and 75 °C led to narrow disperse microspheres with 13.0 and 15.4 micron diameter and homogeneous internal structures, analogous to those reported previously.[19]

2.4.2 Effect of initial plateau time on relative core/shell sizes

Figure 2 shows 2E8 microspheres formed using different step-up and step-down profiles. In the TEM images, Spurr's resin appears lighter than the microspheres. The liquid Spurr's resin preferentially swells the less crosslinked domains formed at higher temperature, which results in the contrast between cores and shells.

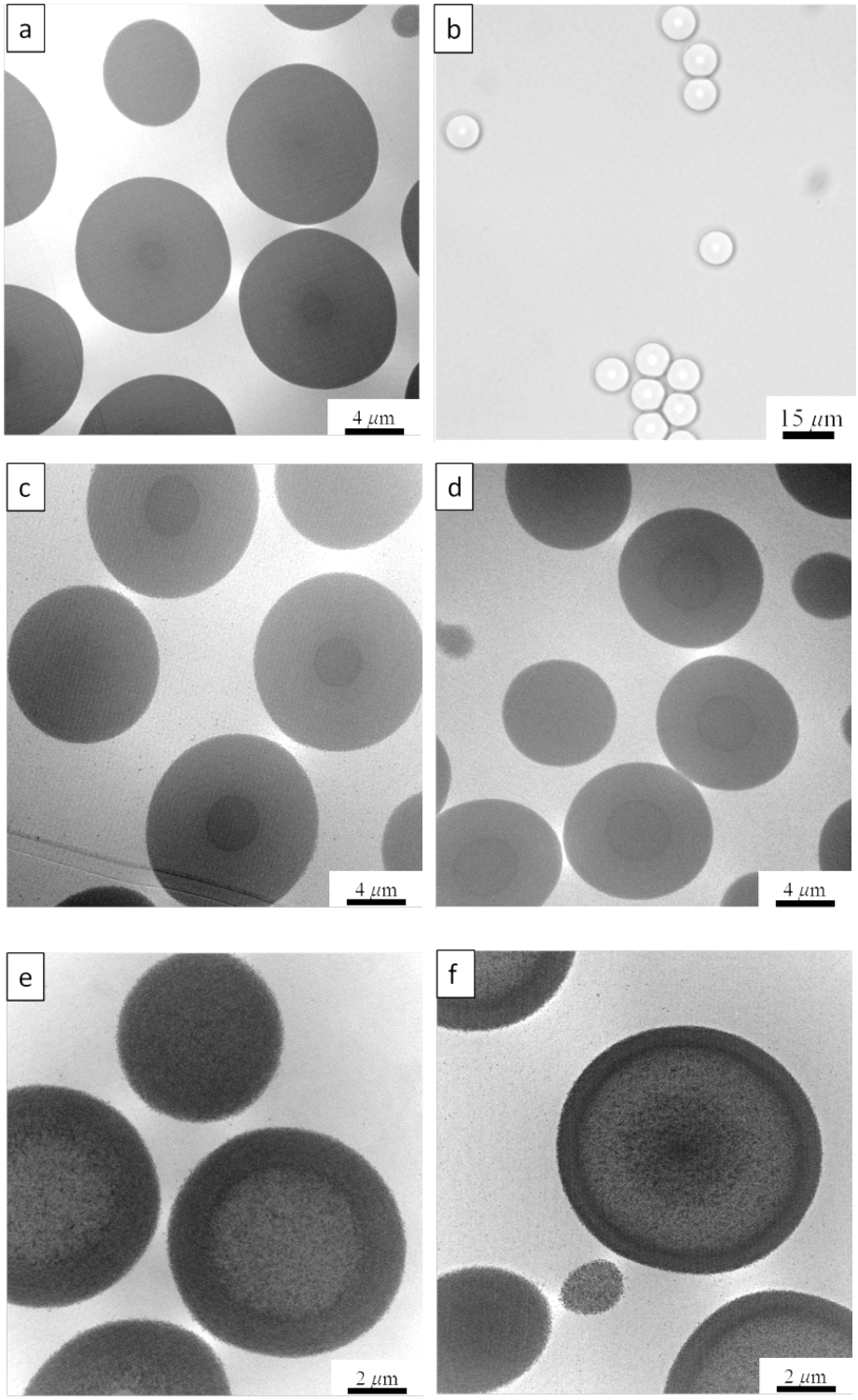

Figure 2. Transmission electron (a, c, d, e, f) and optical microscopy images (b) for microspheres formed with different thermal profiles: 2E8/4 (a and b), 2E8/6 (c) and 2E8/8 (d) for step-up process; 2E8\3 (e) and 2E8\6 (f) for step-down process.

The three step-up samples, 2E8/4 (a), 2E8/6 (c) and 2E8/8 (d), all show a darker inner core corresponding to the initial low temperature (68 °C) period, and a lighter, more resin-swollen outer layer corresponding to the subsequent high temperature (78 °C) polymerization period. These microspheres are all monodisperse, as illustrated in the optical microscope images of 2E8/4 swollen in xylene (b), though only equatorial microtome sections will reveal the denser cores in TEM. The ratios of the inner core diameter to total microsphere diameter increase from 0.23 through 0.33 to 0.42, for 4, 6 and 8 hours initial polymerization periods, respectively, for equatorial cross-sections, in agreement with the expected increase in core diameter with longer low-temperature growths periods. Shell diameter decreases as well during this series, due to decreasing levels of available monomers and initiator and increasing surface area of particles from first period time.

Conversely, the step-down process leads to capsule-like morphologies with swollen cores and denser shells, as seen for 2E8\3 (e) and 2E8\6 (f). Here again the ratio of core diameter to shell diameter increases with longer initial plateau times. Sample 2E8\6 (f), with longer initial high temp period, has dark central cores attributed to onset of core-desolvation by the continuous crosslinking within the growing in lightly crosslinked cores. The resulting dense core area increases in size when the initial high temperature period is extended to 8 hrs (image not shown).

The availability of monomer and initiator in the second period depends on the

length and temperature of the initial period. The core / shell diameter ratios are a complex function of these variables, and not further investigated here.

2.4.3 Effect of monomer loading at constant total crosslinker loading

Increasing the total monomer loading (3E8 or 4E8) or increasing the crosslink percentage (2E9 and 2E10) led to higher crosslink density in both cores and shells, and hence loss of differential swellability and loss of contrast in optical and TEM images (not shown). Instead, we explored increasing monovinyl content while keeping the absolute crosslinker level constant. For example, sample 3E5/8 started with 3 vol.% total monomer loading of which 5.3 vol.% was *m/p*-divinylbenzene - an amount of effective crosslinker identical to that used in 2E8 samples.

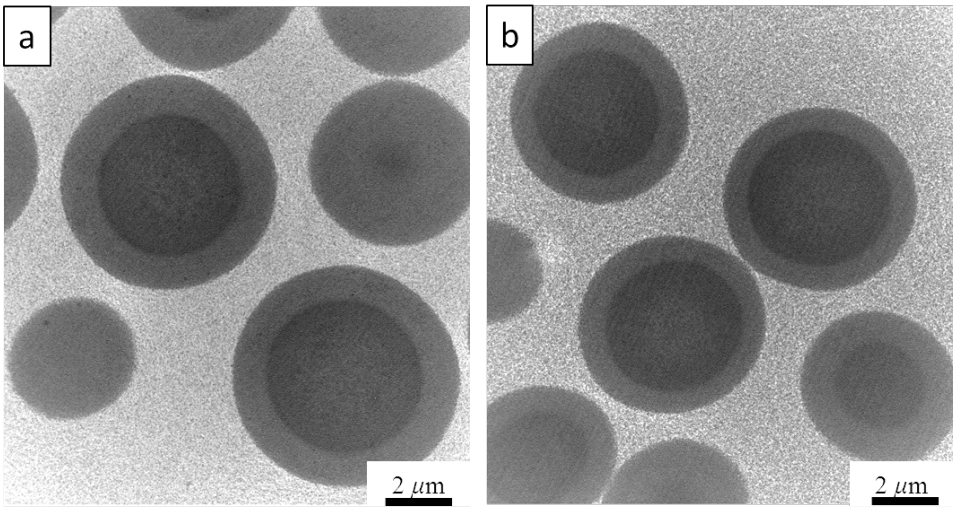

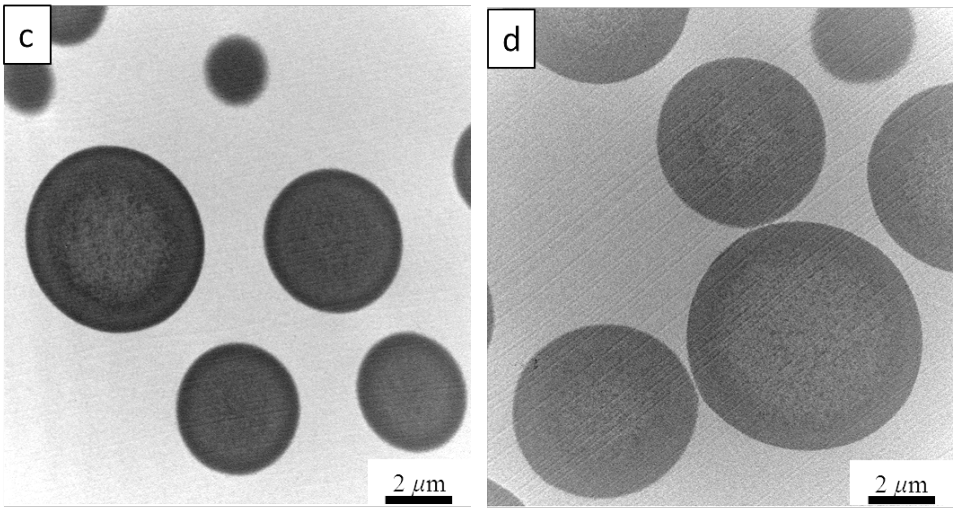

Figure 3. TEM images of microspheres prepared with higher monovinyl content: 3E5/8 (a), 4E4/8 (b) for step-up process; 3E5\8 (c) and 4E4\8 (d) for step-down process.

The resulting step-up microspheres 3E5/8 and 4E4/8 (Fig.3 a and b) show better core-shell contrast than the corresponding 2E8/8 microspheres shown in Fig. 2d. This is attributed to longer kinetic chain lengths and hence more effective network formation, especially during formation of the dense cores in the initial period of the polymerization.

In contrast, the step-down microspheres 3E5\8 and 4E4\8 (Fig.3 c and d) show core-shell contrasts that are roughly comparable to those seen in the corresponding 2E8\3 and 2E8\6 microspheres in Fig. 2 e and f.

2.4.4 Microsphere size characterization

Table 1 shows the average diameters of different types of microspheres swollen in xylenes, determined by optical microscopy. Overall, the diameters are seen to

decrease with increasing total monomer loading (2E8 to 4E8) and for increasing monovinyl monomer loading (2E8, 3E5, 4E4), for both step-up and step-down profiles. The xylene-swollen microspheres are generally about one micron larger than the dry counterparts, which hence show similar diameter trends. These trends are likely due to a larger number of colloidal stable particles present at the end of particle nucleation at higher monomer loadings, which translates into more, but smaller, final microspheres.

Table 1. Average diameters of xylene-swollen microspheres as determined from optical microscopy

Sample (step-up)	Particle diameters (μm)	Sample (step-down)	Particle diameters (μm)
2E8/8	13.2	2E8\8	12.4
3E8/8	12.1	3E8\8	11.2
4E8/8	10.9	4E8\8	11.0
3E5/8	10.0	3E5\8	8.2
4E4/8	8.9	4E4\8	10.6

In many of the polymerizations, some solid polymer was found to deposit on the inner glass walls of the reaction vials. Treating the glass vials with a commercial polydimethylsiloxane-based fomulation, Rain-X^{TM}, reduced wall deposition, and led to final particles with somewhat smaller diameters, presumably through decreased

capture of polymer nuclei (see S5). Internal particle morphology was not affected by these wall effects.

2.4.5 Copolymer composition change

Solution-state proton NMR was used to compare nanogels and final microspheres to the initial comonomer mixture. This was done to test whether the low crosslink density, especially at the oligmer state about two hours into the copolymerization, would allow for solution state signals from surface grafts and other mobile sections of the nanogel network, when swollen in $CDCl_3$.

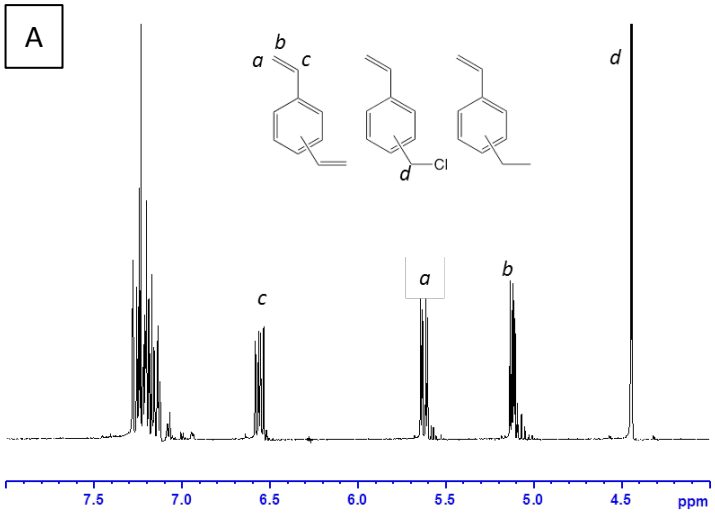

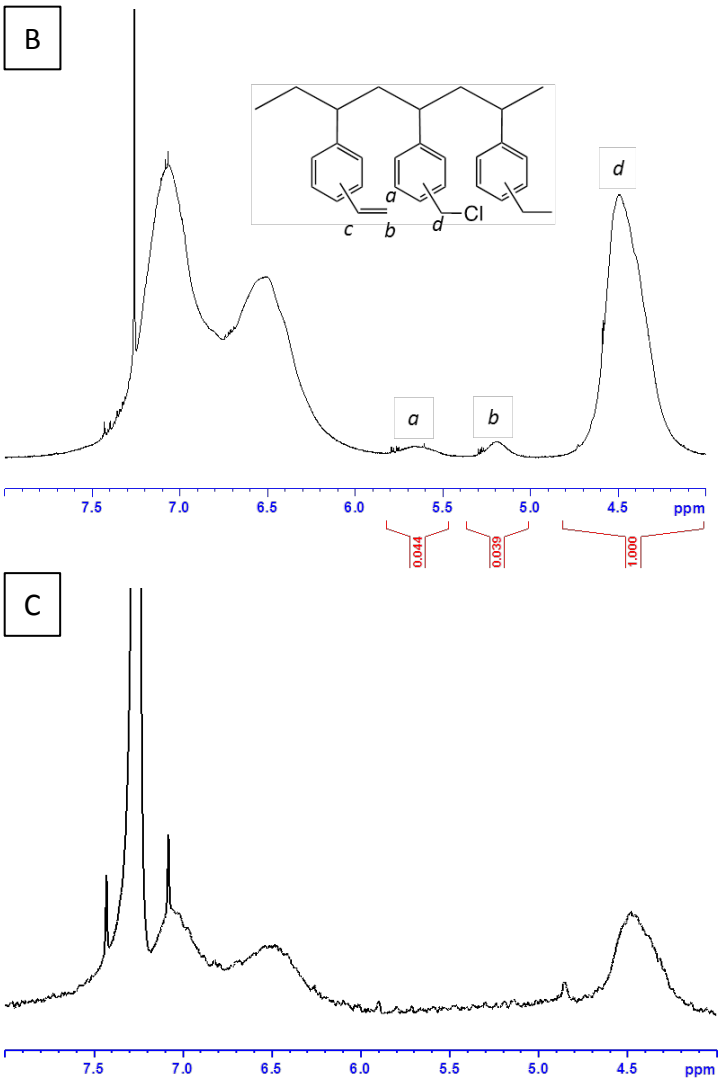

Figure 4. A: Proton NMR spectrum of sample 2E8 0h (monomer mixture); B: Proton NMR spectrum of nanogel sample 2E8 (75) 2h; C: Proton NMR spectrum of 2E8\6 particles. All spectra were recorded in $CDCl_3$, spectra C was processed using 5 Hz line-broadening.

Fig. 4 shows 600 MHz 1H NMR spectra of the initial comonomer mixture corresponding to 2E8, as well as of the corresponding nanogels and microspheres isolated after 2 and 22 hrs of polymerization, respectively. For simplicity, the aliphatic section of the spectra, including signals both from the polymer backbone and the ethyl substituents in DVB-55, are not shown.

Comparison of Fig. 4 A and B shows that the oligomers present after two hours still contain significant NMR-visible vinyl signal at 5.65 and 5.2 ppm, corresponding to the two distinct CH_2 protons of pendant vinyl groups. Clearly visible as well is the strong methylene signal from the pendant chloromethyl groups of CMS, at 4.45 ppm. Comparison of their peak areas indicates that the ratio of vinyl group to chloromethyl groups has only marginally decreased from about 0.09 to 0.07, suggesting that the majority of the pendant vinyl groups are still available for subsequent reaction at this stage. Analogous 2E8 oligomers isolated after three and four hours of copolymerization show small decreases in pendant vinyl/chloromethyl signals (S2 proton NMR). Fig. 4 C, reflecting the final microspheres isolated after 22 hrs of polymerization, only shows a broad peak corresponding to some of the more mobile chloromethyl groups, but no more distinguishable signals for vinyl groups, in agreement with further crosslinking and lower mobility of the polymer network in the final microspheres.

2.4.6 Temperature dependence of Solvation of Model Nanogels

The growth and colloidal stabilization of these polymer microspheres is thought to involve a thin, lightly crosslinked, self-renewing gel layer present at the surface of the growing microspheres. During polymerization, the gel layer covalently captures oligomers and nanogels from solution, and at the same time is converted into solid

polymer by interior crosslinking and desolvation.

In thermally-induced precipitation polymerizations, the colloidal stability of the growing microspheres of the present type is attributed to sufficient solvation of this outer gel layer in acetonitrile at 65 ^{o}C to 78 ^{o}C. Indeed, we have noted that both PDVB55 microspheres as well as DVB55 / CMS copolymer microspheres remain colloidally stable in hot acetonitrile after completion of the polymerization, but reversibly aggregate upon cooling the reaction mixture to room temperature. As the surface gel layer is too thin to be directly observable by TEM or optical microscopy, we prepared model nanogel particles by stopping a 2E8 (70 °C) polymerization after 2, 3 and 4 hrs, close to the onset of particle nucleation. With increasing polymerization from 2 hrs to 4 hrs, about 20 mg to 50 mg oligomers/nanogel particles were isolated for each sample. The isolated polymer consists largely of lightly crosslinked oligomers and nanogel particles with composition and properties similar to the surface gel layer during the microsphere growth period. Fig. 5a shows the plots of turbidity versus temperature for dispersions of 2E8 (70 °C) 2 hrs nanogels in neat acetonitrile (blue hollow squares), in acetonitrile containing 2 vol.% xylene as stand-in for the residual monomers present during polymerization (black hollow circles), and in acetonitrile containing 5 vol.% methanol (red hollow triangles), while Fig. 5b compares transmissivity versus temperature plots for 2E8 (70 °C) nanogels isolated after 2, 3 and 4 hrs of polymerization, all in neat

acetonitrile.

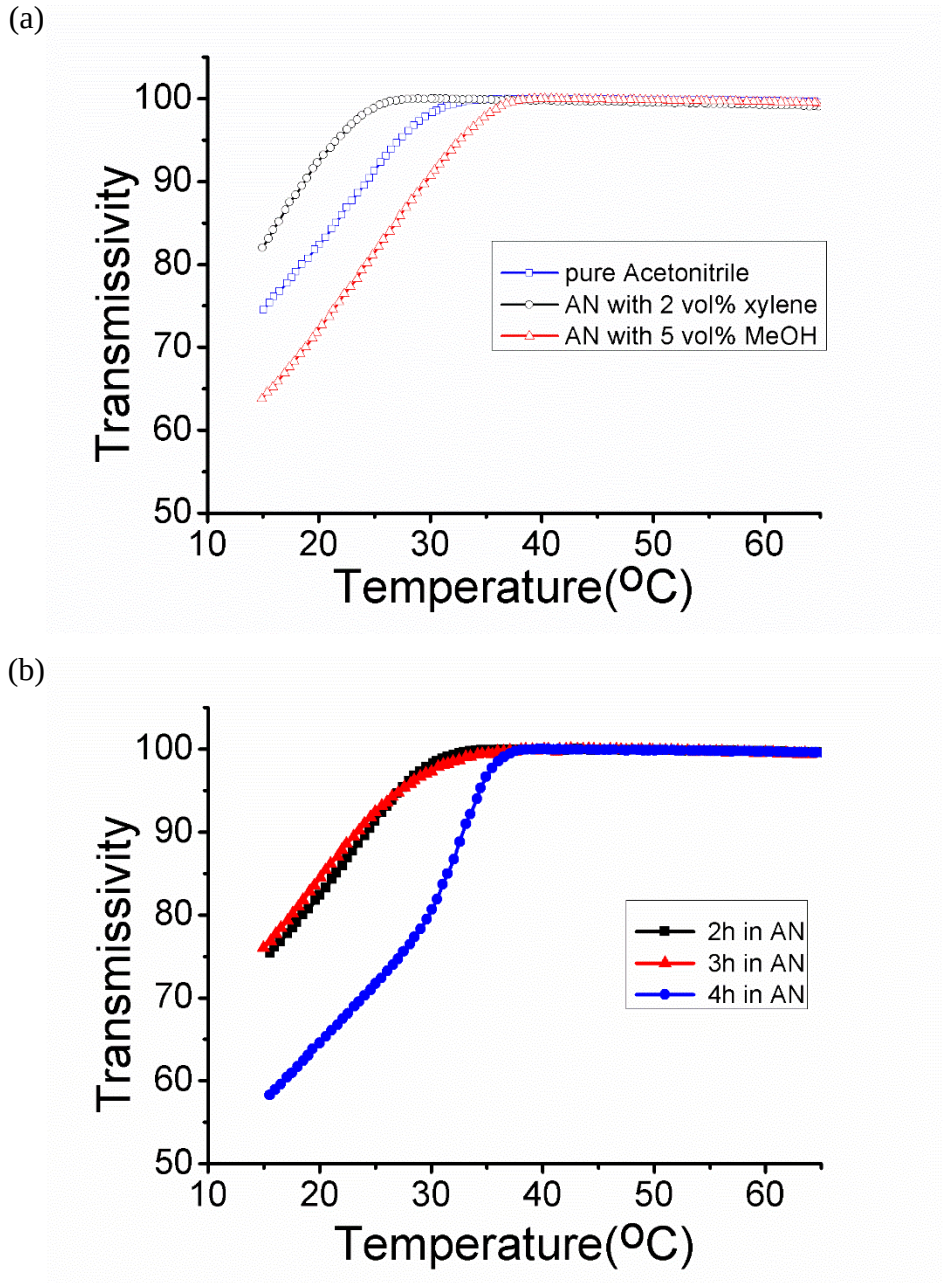

Figure 5. Transmissivity versus temperature plots for dispersions of 2E8 nanogels (oligomers): a) isolated after 2 hrs of polymerization, in neat acetonitrile (blue hollow squares), acetonitrile with 2 vol.% xylene (black hollow circles), and acetonitrile with 5 vol.% methanol (red hollow triangles); (b) isolated after 2 hrs (black square), 3 hrs (red triangle), and 4 hrs (blue round) of polymerization, all in neat acetonitrile.

All thermal runs were carried out from 65 °C down to 15 °C, at 1 °C/min. Fig.

5a shows how the nanogel dispersion in acetonitrile remains clear down to about 30 °C, below which transmissivity decreases. Presence of 2 vol.% xylene helps the nanogels remain colloidally stable down to about 25 °C, while addition of 5 vol.% methanol shifts the onset of turbidity up to about 35 °C. Decrease of transmissivity likely due to both desolvation and aggregation of the individual nanogels. While the resulting aggregates all re-dispersed upon heating, the corresponding transmissivity curves showed considerable variation attributed to slow chain disentanglement, and are hence not shown.

Fig. 5b shows analogous cooling curves for 2E8 (70 °C) nanogels isolated after 2, 3 and 4 hrs, all in neat acetonitrile. It appears that the onset of aggregation moves to higher temperatures, for the same mass-based concentration of nanogels, reflecting possibly a higher degree of internal crosslinking of these ‘older’ nanogels.

The dispersion (δ_d), dipolar (δ_p), and hydrogen-bonding (δ_h) Hansen solubility parameters allow semi-quantitative analysis of the solvent effects shown in 5a. Polystyrene has δ_d = 18.5, δ_p = 4.5, δ_h = 2.9, and poly(DVB-co-CMS) is assumed to have similar values. Neat acetonitrile (δ_d =15.3, δ_p = 18, δ_h = 6.1) is considered a marginal solvent for polystyrene, largely due to its high polarity as reflected by δ_p. The data in Fig. 5a shows acetonitrile to be a non-solvent at room temperature, but to become a solvent for the model nanogels above about 30 °C. The higher

swellability of polymer networks formed at 75 °C and 78 °C, compared with 65 °C and 68 °C, indicate that acetonitrile's solvency for the present styrenic polymers continues to increase from 30 °C to 78 °C.

Addition of xylene is seen to shift the clearing point of the transmissivity curves in Fig. 5a to lower temperatures, while addition of methanol is seen to increase the clearing temperature. These observations are in agreement with xylene (δ_d = 17.6, δ_p = 1, δ_h = 3.1) being a near perfect solvent for polystyrene and related copolymers, while methanol (δ_d = 14.7, δ_p = 12.3, δ_h = 22.3) is a well-known non-solvent for polystyrene, attributable to its mismatch in both polarity and hydrogen-bonding ability.

Scheme 1 summarizes the temperature-dependent polymer-solvent interactions of the model nanogels, and by extension, of the growing microspheres. At 15 °C, nanogels as well as microsphere surface layers are desolvated and aggregated. Increasing the temperature enhances network solvation and causes chain expansion until a clear dispersion of swollen nanogels is obtained at about 30 °C, for neat acetonitrile. Above this temperature, the nanogel dispersions remain transparent, though presumably the coil expansion further increases. This process can be used for thermal inscription into growing CMS/DVB microspheres, by cycling the polymerization temperature between 65 °C and 78 °C which leads to deposition of

corresponding layers with lower and higher swellability (higher and lower crosslink densities).

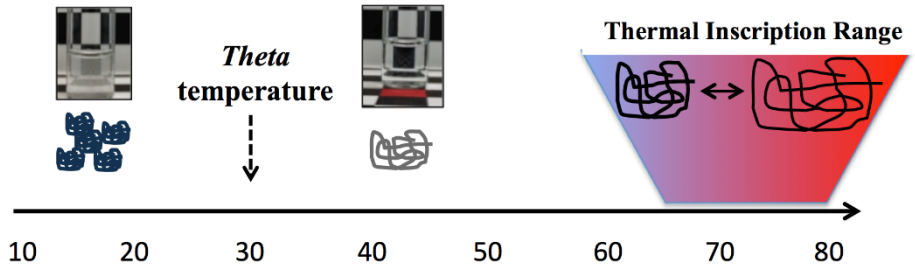

Scheme 1. Oligomer network expansion at different temperature

This suggests that the *theta* temperature for the poly(DVB-*co*-CMS) copolymer is close to 30 °C. This finding is in agreement with the colloidal stability of poly(DVB) microspheres formed using photochemical initiation at 2 - 10 vol.% monomer loading [3]. Though formally carried out at room temperature, Irgum reported the actual polymerization temperatures to be around 30 °C – 32 °C, due to some photo-heating.[21] This suggests that thermal inscription into growing microspheres of the current composition may be carried out by cycling the temperature between 35 °C and 78 °C, provided that radical initiation at low temperature can be supplied through photochemical means, using, *e.g.*, alpha-hydroxy ketones.

Perhaps importantly, the above model experiments point to the use of thermal turbidimetry scans of nanogels or linear copolymers, to screen for suitable temperature/solvent/comonomer combinations for thermally inscribed internal

structures.

In future work, we will carry out photo-initiated precipitation copolymerizations at different temperatures to correlate the results of thermal scans as shown above, with the corresponding precipitation polymerizations. Subsequently, we will use the same approach to explore thermal inscriptions into DVB-only microspheres as well as methacrylate-based systems.

2.5 Conclusion

Thermal profiles during precipitation polymerizations in acetonitrile were used to form crosslinked, mono-disperse poly(divinylbenzene-55-*co*-chloromethylstyrene) microspheres with different core / shell structures. Polymerization temperature was increased from 68 °C to 78 °C during the step-up process, and decreased from 75 °C to 65 °C during the step-down process, with different initial plateau times. The inner structures of the resulting microspheres were explored by TEM of ultramicrotomed samples swollen and embedded in Spurr's resin. With increasing initial plateau time, a larger core and thinner shell structures were observed for both temperature processes. Turbidimetry tests were showed temperature-dependent aggregation/desolvation of corresponding model nanogels in acetonitrile.

By gaining a better fundamental understanding of using temperature changes

during network formation near the *theta* temperature, thermal profiles may be applied to other precipitation polymer system in future.

Acknowledgements

We thank Natural Sciences and Engineering Research Council (NSERC) CREATE programs for financially supporting this project. We thank the McMaster University Electron Microscopy facility and Marcia Reid for help in TEM sample preparation.

2.6 Reference

1. Li, K. and H.D. Stöver, *Synthesis of monodisperse poly (divinylbenzene) microspheres.* Journal of Polymer Science Part A: Polymer Chemistry, 1993. **31**(13): p. 3257-3263.
2. Bai, F., X. Yang, and W. Huang, *Synthesis of narrow or monodisperse poly (divinylbenzene) microspheres by distillation-precipitation polymerization.* Macromolecules, 2004. **37**(26): p. 9746-9752.
3. Limé, F. and K. Irgum, *Monodisperse polymeric particles by photoinitiated precipitation polymerization.* Macromolecules, 2007. **40**(6): p. 1962-1968.
4. Downey, J.S., et al., *Growth mechanism of poly (divinylbenzene) microspheres in precipitation polymerization.* Macromolecules, 1999. **32**(9): p. 2838-2844.
5. Li, W.H., K. Li, and H.D. Stöver, *Monodisperse poly (chloromethylstyrene-co-divinylbenzene) microspheres by precipitation polymerization.* Journal of Polymer Science Part A: Polymer Chemistry, 1999. **37**(14): p. 2295-2303.
6. Frank, R.S., J.S. Downey, and H. Stöver, *Synthesis of divinylbenzene–maleic anhydride microspheres using precipitation polymerization.* Journal of Polymer Science Part A: Polymer Chemistry, 1998. **36**(13): p. 2223-2227.
7. Frank, R.S., et al., *Poly (divinylbenzene-alt-maleic anhydride) microgels: intermediates to microspheres and macrogels in cross-linking copolymerization.* Macromolecules, 2002. **35**(7): p. 2728-2735.

8. Li, W.H. and H.D. Stöver, *Mono-or narrow disperse poly (methacrylate-co-divinylbenzene) microspheres by precipitation polymerization.* Journal of Polymer Science Part A: Polymer Chemistry, 1999. **37**(15): p. 2899-2907.
9. Zhao, L., F. Zhao, and B. Zeng, *Preparation of surface-imprinted polymer grafted with water-compatible external layer via RAFT precipitation polymerization for highly selective and sensitive electrochemical determination of brucine.* Biosensors and Bioelectronics, 2014. **60**: p. 71-76.
10. Bai, F., et al., *Monodisperse hydrophilic polymer microspheres having carboxylic acid groups prepared by distillation precipitation polymerization.* Polymer, 2006. **47**(16): p. 5775-5784.
11. Yan, Q., et al., *Precipitation polymerization in acetic acid: synthesis of monodisperse cross-linked poly (divinylbenzene) microspheres.* The Journal of Physical Chemistry B, 2008. **112**(23): p. 6914-6922.
12. Goh, E.C. and H.D. Stöver, *Cross-linked poly (methacrylic acid-co-poly (ethylene oxide) methyl ether methacrylate) microspheres and microgels prepared by precipitation polymerization: A morphology study.* Macromolecules, 2002. **35**(27): p. 9983-9989.
13. Zheng, G. and H.D. Stöver, *Grafting of poly (alkyl (meth) acrylates) from swellable poly (DVB80-co-HEMA) microspheres by atom transfer radical polymerization.* Macromolecules, 2002. **35**(20): p. 7612-7619.
14. Barner, L., et al., *Synthesis of core-shell poly (divinylbenzene) microspheres via reversible addition fragmentation chain transfer graft polymerization of styrene.* Journal of Polymer Science Part A: Polymer Chemistry, 2004. **42**(20): p. 5067-5076.
15. Li, W.-H. and H.D. Stöver, *Monodisperse cross-linked core-shell polymer microspheres by precipitation polymerization.* Macromolecules, 2000. **33**(12): p. 4354-4360.
16. Li, G., X. Yang, and F. Bai, *A facile route to poly (divinylbenzene) hollow microspheres with pyridyl group on the interior surface.* Polymer, 2007. **48**(11): p. 3074-3081.
17. Ghosh Chaudhuri, R. and S. Paria, *Core/shell nanoparticles: classes, properties, synthesis mechanisms, characterization, and applications.* Chemical reviews, 2011. **112**(4): p. 2373-2433.
18. Li, G.L., H. Möhwald, and D.G. Shchukin, *Precipitation polymerization for fabrication of complex core–shell hybrid particles and hollow structures.* Chemical Society Reviews, 2013. **42**(8): p. 3628-3646.
19. Takekoh, R., et al., *Multilayered polymer microspheres by thermal imprinting during microsphere growth.* Journal of the American Chemical Society, 2006. **128**(1): p. 240-244.
20. Tanaka, T., N. Saito, and M. Okubo, *Control of Layer Thickness of Onionlike*

Multilayered Composite Polymer Particles Prepared by the Solvent Evaporation Method†. Macromolecules, 2009. **42**(19): p. 7423-7429.

21. Lime, F. and K. Irgum, *Preparation of divinylbenzene and divinylbenzene-co-glycidyl methacrylate particles by photoinitiated precipitation polymerization in different solvent mixtures.* Macromolecules, 2009. **42**(13): p. 4436-4442.

2.7 Supporting Information

The temperature changes during both step-up and step-down profiles take finite amounts of time, and the rate of temperature change may affect internal structure. We hence determined the actual temperature profiles during the step-up and step-down processes, using a mercury thermometer inserted into a reaction vessel containing 20 mL water. The results (Figure S1) indicate that temperature change in our system required 30 to 35 minutes, which is considered sufficiently short given the duration of the polymerization segments at constant temperatures. Note that these temperature change times are upper limits, as the heat capacity of water is almost twice that of acetonitrile.

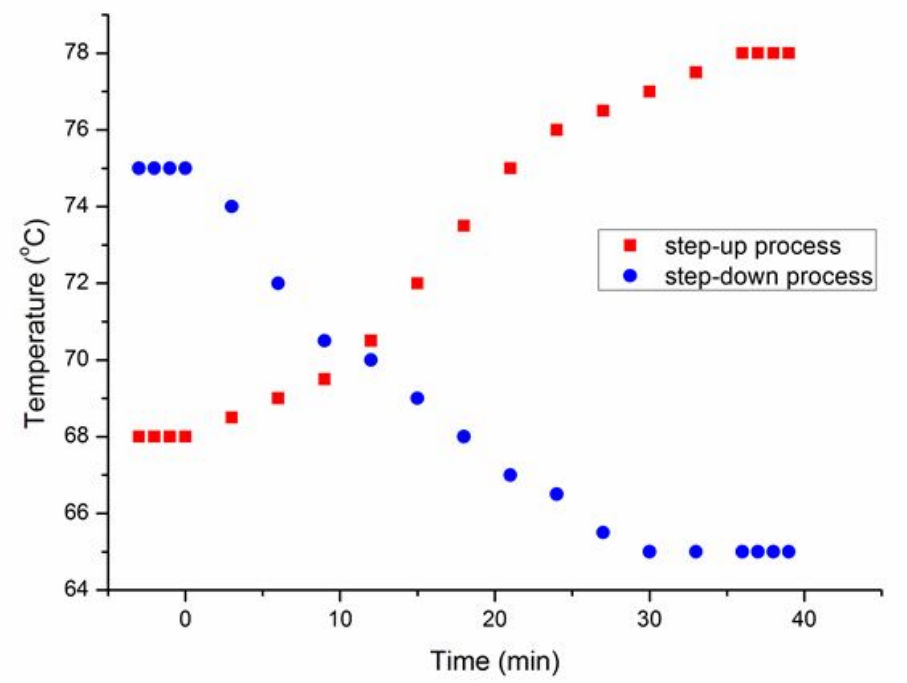

Figure S1. Actual temperature profiles for step-up and step-down processes, as measured using a mercury thermometer inserted into a reaction vial filled with 20 mL of water (not acetonitrile).

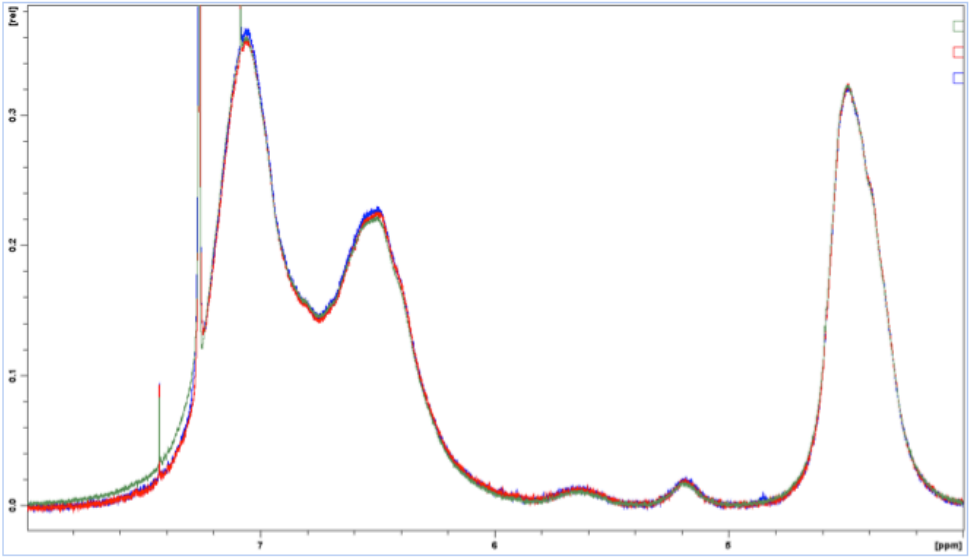

Fgiure S2 Proton NMR spectrum of sample 2E8 (70) 2 h (blue curve), 3 h (red curve) and 4 h (green curve) in $CDCl_3$.

Table S3 Particle yield

Sample	Weight (mg)	Yield (mass/total monomer mass)
2E8(6↑14)	50.7	12.1%
2E8(8↓14)	14.3	3.4%
3E5(8↑14)	58	9.1%
3E5(8↓14)	81	12.8%
4E4(8↑14)	42	5.3%
4E4(8↓14)	111	14.1%

Effect of monomer loading on microspheres

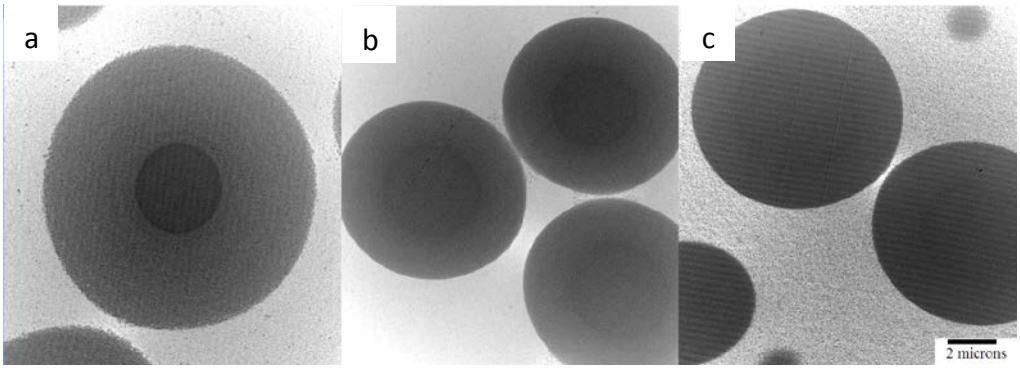

Figure S4 Transmission electron micrographs for copolymer microspheres with different monomer loadings: 2E8 (6/14) (a), 3E8 (6/14) (b) and 4E8 (6/14) (c). All images were taken under 10k magnification. The scale bar is 2 microns.

In Figure S4 (a), clear inner structures were examined in detail for 2E8(6/14) samples for step-up process. The shell of the step-up particles is shown lighter than

the core, indicating relatively lower volumetric intensity of polymer (CMS) in the swollen shell in contrast to the core. The Spurr's resin acts as a solvent before gelation and selectively swells the less crosslinked the shell, resulting in the morphological contrast. It was found that sample with increasing total monomer loading revealed continuously reduced contrast between core and shell part, as shown in Fig. S4 (b) and (c). Microspheres with step-down process show similar result. The chlorine abundance is directly related to CMS intensity. The greyscale distribution in TEM image of polymer microsphere is a direct indicator illustrating the relative intensity of CMS residue.

Wall Effect on Particle Diameter

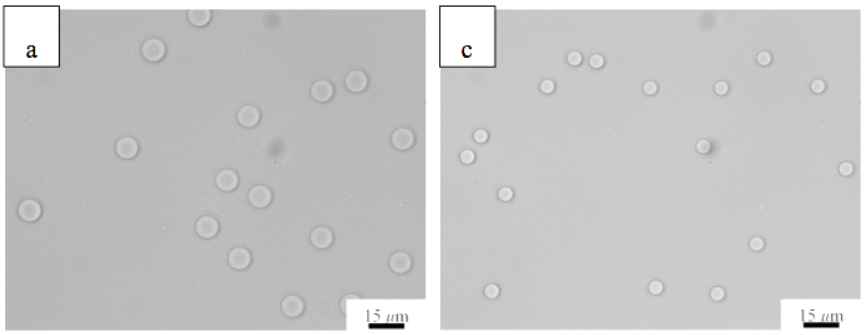

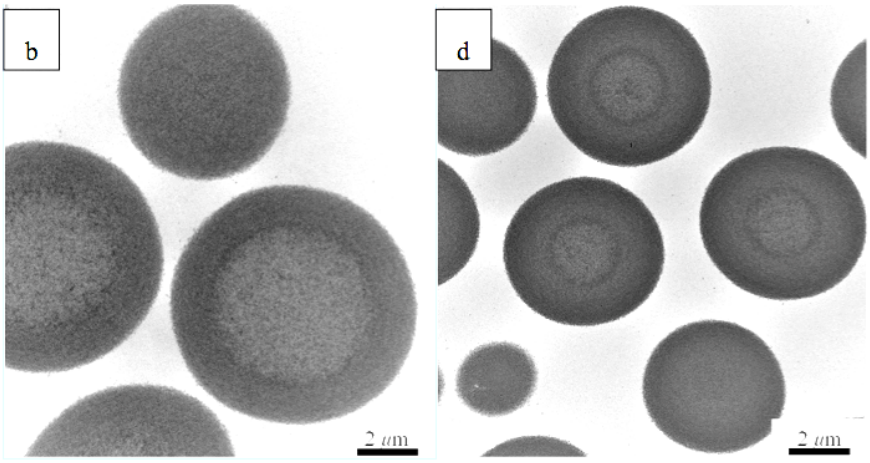

Figure S5. Comparison of copolymer microspheres 2E8(3\14) using: original vials (a) optical microscopic images, (b) Transmission electron micrographs; and pre-treated vials (c) optical microscopic images, (d) Transmission electron micrographs.

During many polymerizations, variable amounts of solid polymer were seen to deposit on the inner surface of the glass reaction vials during the reaction. The removal of polymer nuclei from the reaction medium during the nucleation stage could lead to extended nucleation periods, and hence broader final particle size distributions. Conversely, removal of nuclei and small particles after the nucleation period is complete could lead to enhanced growth of the remaining nuclei, and thus lead to larger final microspheres.

As a result, the reaction vials were pre-treated with a commercial grade polysiloxane (Rain-X ™) in order to try to reduce polymer deposition, and gauge the effect on polymer deposition, particle size and particle size distribution. Treatment with Rain-X ™ was found to significantly reduce wall deposition. Figure S5 shows optical microscopy and TEM images of 2E8\6-14 microspheres formed in glass vials with and without this pre-treatment. Both samples show narrow-dispersed spherical

particles, indicating that polymer deposition on the wall did not lead to a longer particle nucleation period. Final microsphere diameters in pretreated vials were significantly smaller, indicating that more particle nuclei grew into final micropsheres. Both types of microspheres show the expected internal core-shell structure imprinted by the step-up profile.

These results reflect the important role of particle nucleation in precipitation polymerization, and suggest that controlling the number of nuclei at the end of the nucleation period can strongly influence the final microsphere size, and this feature will be explored in a future study.

CHAPTER THREE

3 Hydrophilization of Poly(DVB-*co*-CMS) Microspheres: Preliminary Experiments using Cysteine

3.1 Introduction

In addition to controlling the inner structure, the surface of the particles can be functionalized to gain appropriate hydrophilicity, which is crucial to biocompatibility. Residual vinyl and chlorine groups on DVB/CMS particle surfaces allow further surface modifications[1-3] to form hydrophilic microspheres. The product hydrophilic particles of high uniformity may allow applications as particle scaffolds for ECM (discussed in Section 1.4.3). A series of early publications have focused on applying hydrophilic particles in biomedical applications.[4-6]

One example is post-treatment of polymer microspheres with alkaline $KMnO_4$, which is a strong oxidation agent capable of oxidizing the chloromethyl and residual vinyl groups into carboxylate groups. The manganese oxide residues may require acid treatment to be removed. However, using strong oxidation agents may break polymer backbones and in turn undermine particle integrity. Another problem is the incompatible miscibility between the alkaline $KMnO_4$ (hydrophilic) and DVB/CMS particles (hydrophobic).

Zwitterions, overall neutral molecules with positive and negative charges within

the same molecule, such as amino acids, are a promising route to hydrophilization. For example, cysteine thiols are actively involved in protein functions[7, 8] and can be an ideal candidate for hydrophilization of the present DVB/CMS particles. Substitution of the polymer-bound chlorine by cysteine-thiol groups would introduce amine / carboxylic zwitterions.

Overall, the chlorine groups on the particle surface are easy to be substituted with a good nucleophile (eg. amine). As a common functionalization method in preparing ion exchange resins [9-11], the poly(DVB-*co*-CMS) microspheres can also be treated with trimethylamine (TEA). The reaction is based on the nucleophilic attack of amine to chlorine group particle surface. As a result, the chlorine groups can form highly hydrophilic quaternary ammonium cations. However, it needs to be considered that such ammonium cations can be toxic to cells.

The p*K*a of cysteine depends on the equilibrium between thiol and thiolate, and affect the reactivity and nucleophilicity[12] and the value is close to 8.6 in aqueous solution[13, 14]. Under basic condition, the sulfur group can deprotonate preferentially over primary ammonium cations (pKa ~10), and thiolate is a very strong nucleophile[3, 15]. It acts as a good nucleophile substituting the chloro group on CMS.[16] As a result, preliminary work, described below, focused on using cysteine as nucleophile in DMF.

3.2 Experimental

3.2.1 Materials

Commercial divinylbenzene-55 (DVB-55, 55 % divinylbenzene isomers, 45 % ethylstyrene isomers, Aldrich Chemical Company Inc.), chloromethylstyrene (CMS, mixture of 3- and 4-isomers, Aldrich), solvents (acetonitrile, HPLC grade, Caledon Labs; methanol, HPLC grade, Caledon Labs; xylenes, certified A.C.S., Fisher Scientific) were used as received. Initiator 2,2'-azobis(2-methylpropionitrile) (AIBN, Dupont) was recrystallized from methanol. For microspheres modification, commercial L-cysteine hydrochloride monohydrate (BioUltra grade, Sigma-Aldrich) and potassium carbonate (reagent grade, Aldrich Chemical Company Inc.) were used as received.

3.2.2 Experiment Procedures

3.2.2.1 Polymerization of homogenous particle

During a precipitation polymerization, DVB-55 and CMS were added to neat acetonitrile to give 20.0 mL of solutions containing 4 vol.% total monomer, of which 4 vol.% were actual crosslinker (3/4-divinylbenzene) relative to total monomer percentage. AIBN initiator was added in an amount corresponding to 2 wt % in respect to total monomer weight. All reactions were performed in 25 mL glass screw cap vials placed in an oven with a set of steel rollers rotating at 4 rpm.

Polymerization temperatures were set around 70 ^{o}C for 22 h.

3.2.2.2 Functionalization of particles with cysteine

After the microsphere isolation, 20 mg dry particles were added to 5 ml dimethylformamide (DMF) with cysteine hydrochloride monohydrate (fivefold molar excess). Excess anhydrous solid K_2CO_3 was added to the reaction mixture. The reaction was heated at 65 ^{o}C overnight under stirring. Reaction supernatant was removed and the particles were washed by DI water followed by freeze-drying.

3.2.2.3 Preparation of SEM sample

The original polymer microspheres were suspended in THF and the solution was added to the stub directly. Functionalized dry particle sample was suspended in DI water and few drops of aqueous solution were directly added on the stub. The stubs with particle samples were left on the bench with cover overnight to dry.

3.3 Preliminary results

3.3.1 Surface modification with cysteine salt

CMS/DVB particle 2E8\6 was used as-prepared microspheres treated with cysteine hydrochloride in basic condition. As shown in Figure 3.3.1 (a), the hydrophobic unfunctionalized particles strongly aggregate in water. After

functionalization with cysteine, particles can be easily suspended in water (Fig. 3.3.1 b). Functionalization with cysteine provides a hydrophilic surface and may induce electrosteric stabilization. However, the degree of functionalization and the depth of penetration of cysteine is not clear at this point.

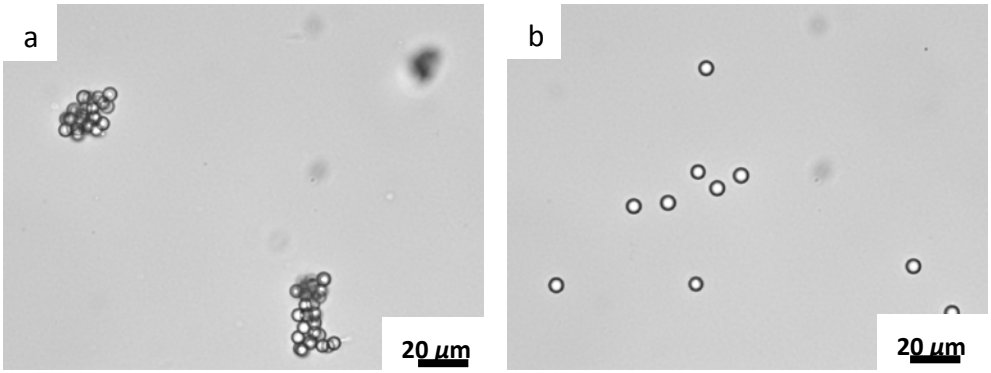

Figure 3.3.1 Optical microscopic images of particle sample 2E8\6 in water before (a) and after (b) functionalization.

3.3.2 SEM/EDS analysis on modified particles

Analogous surface modification was also carried out on non-structured particles 4E4(70). Scanning electron microscopy (SEM) with Energy dispersive X-ray spectroscopy (EDS) was used to detect the elemental composition of cysteine-functionalized particles as shown on Figure 3.3.2. Point detection was repeated for at least five points and same result was obtained. Figure 3.3.2 a and b) shows the SEM image and the EDS spectrum of the original sample, with no sulfur detectable. After functionalization, with cysteine, a significant sulfur peak (energy peak Kα at 2.307) appears at Fig.3.3.2 c,d). Chlorine peaks indicate the existence of residual Cl and suggest fully functionalization is not accomplished. The average ratio

(atomic %) of S to Cl is close to 1 to 2, which indicates one third of the Cl atoms were reacted.

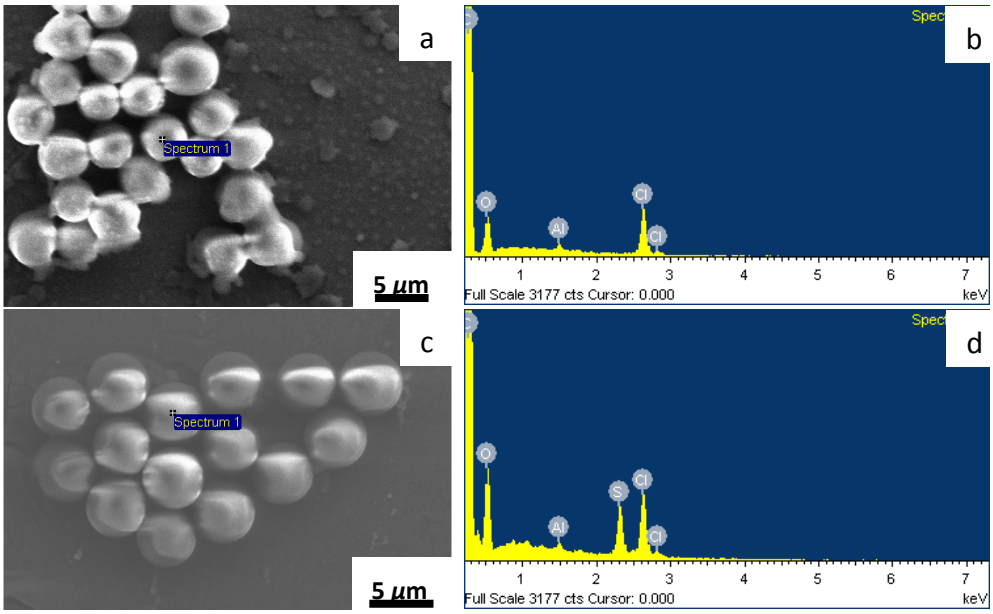

Figure 3.3.2 Typical SEM picture and EDS analysis of a,b) original particle; c,d) functionalized particle

3.3.3 Conclusion

Poly(DVB-*co*-CMS) microspheres were synthesized by precipitation polymerization and then functionalized with cysteine by substitution reaction. Optical microscopic images showed that the ability of functionalized particles suspended in water with no apparent size change. Successful functionalization has been proved by the existence of sulfur in SEM/EDS analysis. However, functionalization may only limit to particles surfaces which would restrict the bio-application to cells. Fully functionalization is ideal to give highly hydrophilic and water swollen particles. The cysteine methylester may provide an alternative reagent

with reduced hydrophilicity. Partial hydrolysis can be carried out after functionalization of particles to obtain desired positive charge density on particle surface.

3.3.4 Reference

1. Kip, Ç., et al., *A new type of monodisperse porous, hydrophilic microspheres with reactive chloroalkyl functionality: synthesis and derivatization properties.* Colloid and Polymer Science, 2014. **292**(1): p. 219-228.
2. Chen, X., et al., *Active Poly(4-chloromethyl styrene)-Functionalized Multiwalled Carbon Nanotubes.* Macromolecular Chemistry and Physics, 2013. **214**(16): p. 1829-1835.
3. Khurana, J.M. and P.K. Sahoo, *Chemoselective Alkylation of Thiols: A Detailed Investigation of Reactions of Thiols with Halides.* Synthetic Communications, 1992. **22**(12): p. 1691-1702.
4. Fleischmann, C., et al., *A robust platform for functional microgels via thiol-ene chemistry with reactive polyether-based nanoparticles.* Polymer Chemistry, 2015.
5. Selvam, S., et al., *Injectable in situ forming xylitol–PEG-based hydrogels for cell encapsulation and delivery.* Colloids and Surfaces B: Biointerfaces, 2015. **126**(0): p. 35-43.
6. Platen, M., et al., *Poly(2-oxazoline)-Based Microgel Particles for Neuronal Cell Culture.* Biomacromolecules, 2015.
7. Marino, S.M. and V.N. Gladyshev, *Cysteine function governs its conservation and degeneration and restricts its utilization on protein surfaces.* Journal of molecular biology, 2010. **404**(5): p. 902-916.
8. Marino, S.M. and V.N. Gladyshev, *Analysis and functional prediction of reactive cysteine residues.* Journal of Biological Chemistry, 2012. **287**(7): p. 4419-4425.
9. Ford, W.T., et al., *Synthesis of monodisperse crosslinked polystyrene latexes containing (vinylbenzyl)trimethylammonium chloride units.* Langmuir, 1993. **9**(7): p. 1698-1703.
10. Sherazi, T.A., et al., *Polyethylene-based radiation grafted anion-exchange membranes for alkaline fuel cells.* Journal of Membrane Science, 2013. **441**(0): p. 148-157.
11. Ezzeldin, H.A., A. Apblett, and G.L. Foutch, *Synthesis and Properties of Anion*

Exchangers Derived from Chloromethyl Styrene Codivinylbenzene and Their Use in Water Treatment. International Journal of Polymer Science, 2010. **2010**: p. 9.

12. Winterbourn, C.C. and D. Metodiewa, *Reactivity of biologically important thiol compounds with superoxide and hydrogen peroxide.* Free Radical Biology and Medicine, 1999. **27**(3): p. 322-328.
13. Haynes, W.M., *CRC handbook of chemistry and physics*. 2014: CRC press.
14. Thurlkill, R.L., et al., *pK values of the ionizable groups of proteins.* Protein science, 2006. **15**(5): p. 1214-1218.
15. Roos, G., N. Foloppe, and J. Messens, *Understanding the p K a of Redox Cysteines: The Key Role of Hydrogen Bonding.* Antioxidants & redox signaling, 2013. **18**(1): p. 94-127.
16. Haigh, D.H. and C.W. Roberts, *Polymers of l-amino acid derivatives of s-(substituted benzyl) compounds*. 1972, Google Patents.

CHAPTER FOUR

4 Conclusion and Future Work

4.1 Conclusion

Structured divinylbenzene-55 (DVB-55) / chloromethylstyrene (CMS) copolymer microspheres have been successfully fabricated by thermal imprinting precipitation polymerization approach. Microspheres were synthesized from DVB-55 / CMS mixtures with 2 to 4 vol.% total monomer loading and 8 to 4 vol.% crosslinker in acetonitrile in two thermal profiles. Step-up thermal profiles, with polymerization temperature increasing from 68 ^{o}C to 78 ^{o}C after 4, 6 and 8 hrs led to dense core / swollen shell morphologies; while, step-down profiles, with polymerization temperature decreasing from 75 ^{o}C to 65 ^{o}C after 3, 6 and 8 hrs led to formation of the inverse, capsular morphologies consisting of swollen cores and dense shells. Such variations in morphology are attributed to the temperature-dependent crosslinking efficiency during particle growing. By control of thermal profile, relative core/shell thickness can be altered.

Optical Microscopy of the isolated particles in good solvents and Transmission Electron Microscopy (TEM) of ultra-microtomed sections of particles embedded in epoxy resin have been used to assess internal particles structure. Inner structures were reflected by regions of different brightness (greyscale) in TEM images. In

addition, turbidity measurements were used to evaluate network properties at different temperature from 65 ^{o}C to 15 ^{o}C. The results reveal the effects of both solvent composition and temperature on polymer swelling ability, and provide an effective approach for future development of thermal imprinting with diverse monomer/solvent combinations.

Hydrophilization of Poly(DVB-*co*-CMS) microspheres were then carried out with cysteine by substitution reaction. Preliminary results of optical microscopic images showed that the ability of functionalized particles suspended in water and SEM/EDS analysis proved the existence of sulfur on functionalized particles. However, functionalization may only limit to particles surfaces which would restrict the bio-application to cells. Detailed study is required for fully control over particle structure and hydrophilicity.

4.2 Future Work

The objective of this thesis is to understand temperature and solvent dependent polymer network formation in the precipitation polymerization of poly(CMS-*co*-DVB) microspheres by thermal imprinting. The understanding of the relationship between polymer and solvent (and/or temperature) may help us to better control polymer particle morphology and fabricate structured hydrophilic microspheres based on diverse monomer/solvent combinations.

4.2.1 Extension of Thermal Imprinting

4.2.1.1 Varying polymerization time for second polymerization stage

The second stage time of DVB/CMS system copolymerization can be altered as shown in Fig.4.2.2.1 with polymerizations all starting at the same time. Generally, longer polymerization time at second stage would lead to thicker shell formation, even though less monomer is available for the shell formation at later stage, and the particle volume is increasing which may slow down the particle size development. Such strategy may allow the control of particle shell thickness independently with same inner structure. By thermal profiling, polymer capsules may also be obtained by step-down process.

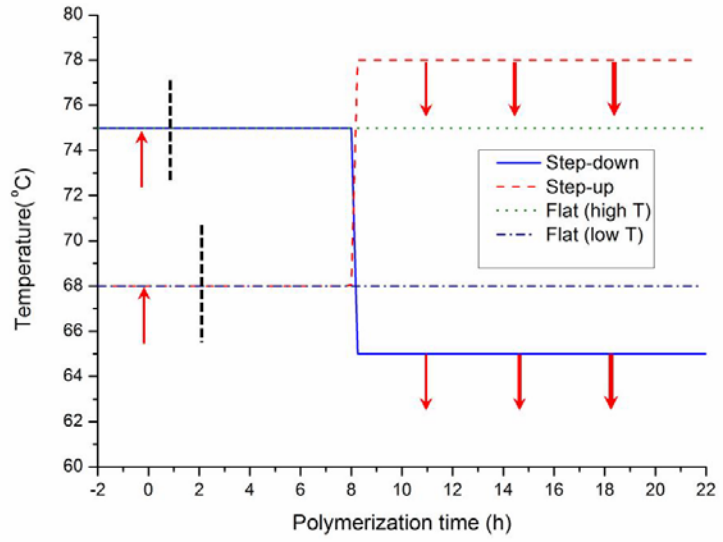

Figure 4.2.1.1. Temperature profiles of step-down (solid line), step-up process (dashed line), flat at high temperature (dotted line), and flat at low temperature (dash dot line). The arrows denote the polymerization starting time for samples with different second stage reaction time.

4.2.1.2 Extending thermal imprinting method to other copolymer systems

The approach to core/shell structure by thermal imprinting should also apply to other monomer/solvent system. This method here provided a simple approach towards construction of inner structured particle with clean surface. The turbidity measurements used in this research can serve as a method to pre-screen proper solvent and temperature conditions for other polymer systems. For certain polymer microsphere system, turbidity measurement on corresponding linear polymer may indicate the *theta* condition, and hence the potential thermal profile temperature range. Hydrophilic copolymer system (i.e. DVB/MAn, MAA/PEGMM/EDMA[1]) are of particular interest for exploration.

4.2.2 Mechanical Characterization

Thermogravimetric Analysis (TGA) and Differential Scanning Calorimetry (DSC) can be used to determinate the glass transition temperature (Tg) and decomposition temperature (Td) of polymer microsphere. Based on Tg and Td, proper characteristic temperature can be reasonably predicted and applied to mechanical test for particle deformation.

Study of nanomechanical properties of single polymer microspheres is of interests.[2] Nano-TA technique based on Atomic Force Microscopy (AFM) allows

measurement of local thermal behavior of materials.[3] It may be applied for Tg measurement on single particles. The different cross-linking density of the structured microspheres may affect the Tg for core and shell part. Compression of particle by nanoimprint lithography[4-6], study of particle deformation under pressure and heating, and its potential to get recovered after released [6] is also attractive for structured microspheres.

4.2.3 Hydrophilic Poly(DVB-*co*-MA) Microsphere

The challenge with hydrophilization of DVB/CMS particles continues to be the mismatch of polarities between as-formed particles and functionalization reagents. One solution relies on incorporation of hydrophilic monomer in particle polymerization process. The work in this thesis may help control thermal structuring of microspheres formed by future precipitation polymerizations of polar comonomers. One example involves poly(DVB-*co*-MAn) particles prepared by precipitation polymerization of DVB and MAn, and microspheres derived from these by hydrolysis or other modifications of the anhydride groups.

A visiting student Jingwen Li, conducted this part of work under my supervision. Preliminary results showed that DVB/MAn particles can be prepared with cross-linker percentage in the range of 3 vol.% to 10 vol.%, at monomer loading of 4 vol.%. MEK/heptane mixed solvent is used where MEK is a good

solvent for copolymer while heptane is a poor solvent. Particles are formed when MEK percentage lies between 50 % and 70 %. With decreasing cross-linking level and increasing MEK percentage, both particle size and softness increase. The result DVB/MAn particles can be hydrolyzed under basic conditions using NaOH aqueous solution. The final poly(DVB-*co*-MA) particles showed varying swelling level at different pH. Larger particles can be obtained with pH ranging from 4 to 10. More fundamental work is required over control of inner structure for its future application as particle scaffolds.

4.2.4 Reference

1. Goh, E.C. and H.D. Stöver, *Cross-linked poly (methacrylic acid-co-poly (ethylene oxide) methyl ether methacrylate) microspheres and microgels prepared by precipitation polymerization: A morphology study.* Macromolecules, 2002. **35**(27): p. 9983-9989.
2. He, J., Z. Zhang, and H. Kristiansen, *Nanomechanical characterization of single micron-sized polymer particles.* Journal of applied polymer science, 2009. **113**(3): p. 1398-1405.
3. Germinario, L., *nano-TA TM: Nano Thermal Analysis.*
4. Soles, C.L. and Y. Ding, *Nanoscale polymer processing.* Science, 2008. **322**(5902): p. 689-690.
5. Wang, Z., et al., *Programmable, Pattern-Memorizing Polymer Surface.* Advanced Materials, 2011. **23**(32): p. 3669-3673.
6. Cox, L.M., et al., *Morphing Metal–Polymer Janus Particles.* Advanced Materials, 2014. **26**(6): p. 899-904.

5 Appendix

5.1 Solvent selection in optical microscopy characterization

As shown in Figure 5.1, optical microscopy images taken in different solvent illustrates the particles topography and their internal structures, based on swelling in (a) xylene and (b) acetone, respectively. Xylene is a much better solvent for the DVB/CMS particles than acetone, thus able to develop the internal morphology by selectively swelling the domain (core: shell) formed at higher temperature. On the other hand, xylene has a refractive index at 1.5 that is much closer to that of the polymer (1.56) than acetone (1.36). Such close match in refractive index hides some of the features of good swelling, leading to more transparent particles with less internal contrast, shown in Fig. 5.1 (a). In comparison, image taken with acetone shows higher contrast due to the larger refractive index difference between acetone (1.35) and the polymer (1.56).

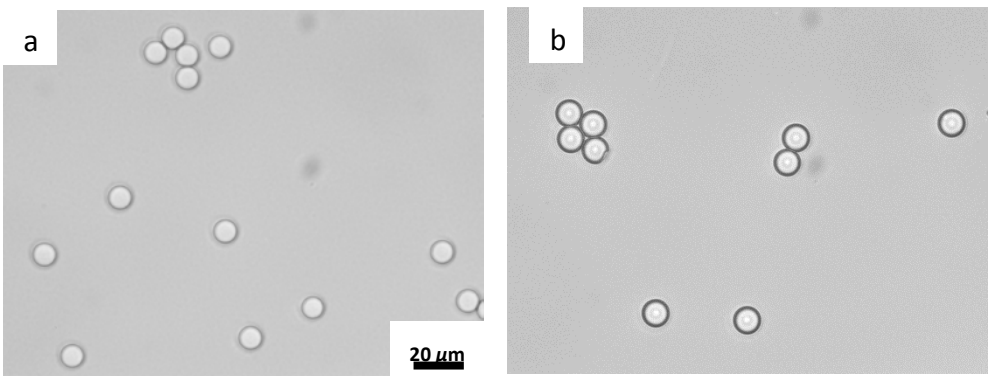

Figure 5.1 Optical microscope images of sample 2E8/4 with different solvent: (a) was

prepared in xylenes which is a relative good solvent for polymer particles; (b) was prepared in acetone.

5.2 Particle size measurement by optical microscopy

As particle assembling along with solvent boundary and drying, the combination of immersed gravity and inter-particle pressure facilitated reallocation to a state of hexagonal repacking, as shown in Figure 5.2. Such repacking pattern is exactly the same to the distribution of a great number of identical steel balls packing in a pool, where the balls tend to form close-packed hexagonal pattern that is mostly energy favored. Consider the scenario that if strong shear is applied in the ball-pool system (e.g. paste highly viscous syrup onto surface of balls and inner surface of pool); it is hardly for the balls to repack in the hexagonal pattern because such reallocation is greatly time-consuming. As a result, we may assert that the perfect hexagonal pattern of polymer microspheres in Figure 5.2 suggests relatively weak shear between different particles; or in other word, relatively weak inter-particle coagulation. In addition, quite a few microspheres exhibited slight deformation, as shown in Figure 5.2. Further experiment showed that re-dispersion of those particles in good solvent allowed them to regain good spherity, indicating that such deformation is elastic.

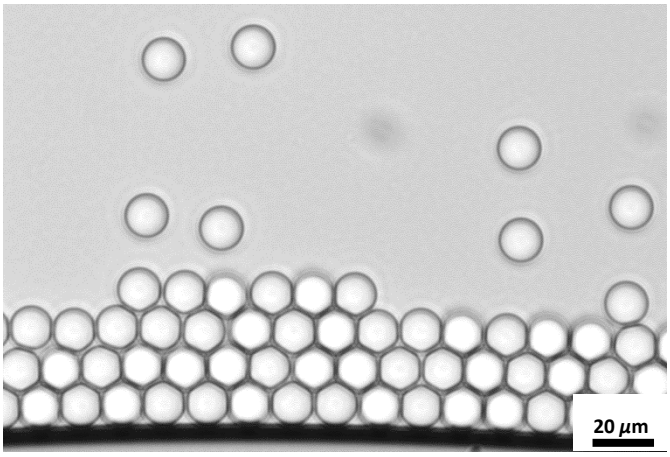

Figure 5.2 Optical microscopic images of sample particles assembling along with solvent boundary and drying.

Comparison of particle diameters regards to the xylene-swollen particles before drying. Particle size may be a time-dependent property due the “wall effect” that was discussed in Chapter 2. General variation of swollen microspheres size with time was investigated in this research. Particle diameters in xylene decrease with increasing cross-linker percentage and monomer loading, which could be explicated by the suppressed particle swellability across the board caused by high crosslink levels. There should be a minimum limit of crosslinker level, below which the crosslinker cannot transform discrete polymers to concrete particle. (Unpublished work)

5.3 Exploration of embedding resin for TEM characterization

In order to obtain better images with higher core/shell contrast, polymer samples in different resins were fabricated. Ideal embedding resin should behave as good solvent for both PDVB and PCMS, with closer solubility parameters δ

($MPa^{1/2}$) to those two (19.3 and 20.3, respectively). In addition, it is obvious that the use of new polymer resins should be chlorine free and allow good contrast in TEM image. Apart from Spurr's resin, another two types of polymer resins were investigated: poly(methyl methacrylate) resin and poly(methyl methacrylate-*co*-methacrylate) (80:20) resin.

5.3.1 Embedding microspheres in polymer resin

TEM samples were also prepared by embedding microspheres in vinylic resins: PMMA resin or poly(MMA-co-MA) (80:20) resin. A typical procedure is similar to that of Spurr's resin: swelling particles in the MMA or MMA/MA monomer containing 1 wt % initiator (i.e. AIBN); curing the mixture at 55 °C for 20 h and then at 80 °C for 1.5h; ultra-microtoming the resin that obtains embedded samples, followed by deposition on 3 mm copper/platinum TEM grids.

5.3.2 TEM characterization of microspheres embedded in polymer resin

Microscopic test suggested that microspheres in MMA give comparable swelling as in xylenes (corresponding solubility parameters are 18, 18.2 and 18, for MMA, MA, and xylenes, respectively). The free radical polymerization of the MMA leads to formation of a highly chlorine-free solid resin, allowing excellent blank background under TEM view. Great efforts have been made in PMMA preparation

and curing to allow PMMA an acceptable intensity and toughness for microtoming, due to the common generations of brittle fractures/cracks during microtoming. Figure 5.3.2 shows the detailed structure of internal structures of microspheres, embedded in two different resins at a high monomer loading (3E8/6).

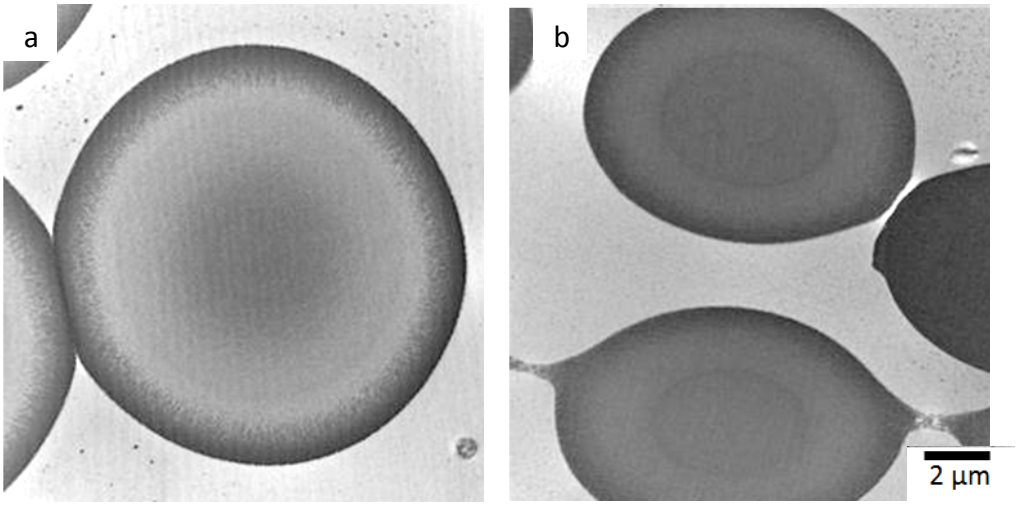

Figure 5.3.2 Transmission electron micrographs for 3E8/6 copolymer microspheres in (a) PMMA resin and (b) Poly(MMA-co-MA) (80:20) resin.

As mentioned previously, dark core with light shell in TEM image was typically observed in step-up process. It was notable that the dark rings shown near particles surfaces have not been clearly understood. Also, PMMA is relatively sensitive to electron beam. The resin sample turn to decompose rapidly when exposed under electron beam in TEM and small-hole defects appeared to accelerate such degradation. The small-holes formation occur during polymerization of MMA due to the initiator. The occasionally observed irregular defects, such as extruded rings, were believed to be caused by sample microtoming. The resin degradation can be a severe problem for observation, which mainly attributes to the relatively low ceiling

temperature of PMMA of around 220 ^{o}C.

Copolymer resin based on poly(MMA-*co*-MA) (80:20) that a portion of MMA was substituted by MA was also investigated as embedding substrate, as shown in Figure 5.4.2 (b). The result showed that such resin allowed improved radiative resistance, which could be explicated by the relatively high ceiling temperature of PMA that suppressed resin decomposition and greatly prolonged the effective observation time. Another interesting phenomenon reflected in TEM test was that the use of poly(MMA-*co*-MA) resin also allowed fewer holes generation.

One major dissimilarity between sample images detected under optical microscopy and TEM relied on the distinct non-spherity of target polymer particles shown in the latter characterization method. Considering the low dosage of both starting monomer and cross-linker, soft particles were expected to form with good swelling ability, low polymer intensity. The sectioning process, as introduced above, introduced particle deformation from high spherity to high irregularity. Embedding resins, especially poly(MMA-*co*-MA) based resins, were not rigid enough to suppress such deformation, resulting in the prolonging direction of particles perpendicular to the knife cutting direction. The long axis of polymer particles was perpendicular to straight lines that were generated by knife slicing. Such phenomena further stressed the interaction between the non-spherity nature of particles and microtoming. The connections bridging two microspheres in Fig. 5.3.2 (b) can be

attributed to lightly cross-linked surface layers formed in resin formation. All the results shown here were consistent with step-down processed samples.